Oil & Gas Science and Technology – Rev. IFP Energies nouvelles **75**, 72 (2020)

https://doi.org/10.2516/ogst/2020066

Available online at:
ogst.ifpenergiesnouvelles.fr

REGULAR ARTICLE OPEN ACCESS

Design and formulation of surfactant stabilized O/W emulsion for application in enhanced oil recovery: effect of pH, salinity and temperature

Narendra Kumar, Saif Ali, Amit Kumar, and Ajay Mandal*

Department of Petroleum Engineering, Indian Institute of Technology (Indian School of Mines), Dhanbad 826 004, India

Received: 8 April 2020 / Accepted: 28 August 2020

Abstract. Mobilization of crude oil from the subsurface porous media by emulsion injection is one of the Chemical Enhanced Oil Recovery (C-EOR) techniques. However, deterioration of emulsion by phase separation under harsh reservoir conditions like high salinity, acidic or alkaline nature and high temperature pose a challenge for the emulsion to be a successful EOR agent. Present study aims at formulation of Oil-in-Water (O/W) emulsion stabilized by Sodium Dodecyl Sulfate (SDS) using the optimum values of independent variables – salinity, pH and temperature. The influence of above parameters on the physiochemical properties of the emulsion such as average droplet size, zeta (ζ) potential, conductivity and rheological properties were investigated to optimize the properties. The influence of complex interactions of independent variables on emulsion characteristics were premeditated by experimental model obtained by Taguchi Orthogonal Array (TOA) method. Accuracy and significance of the experimental model was verified using Analysis Of Variance (ANOVA). Results indicated that the experimental models were significantly ($p < 0.05$) fitted with main influence of salinity (making it a critical variable) followed by its interactions with pH and temperature for all the responses studied for the emulsion properties. No significant difference between the predicted and experimental response values of emulsion ensured the adequacy of the experimental model. Formulated optimized emulsion manifested good stability with 2417.73 nm droplet size, −72.52 mV ζ-potential and a stable rheological (viscosity and viscoelastic) behavior at extensive temperature range. Ultralow Interfacial Tension (IFT) value of 2.22E-05 mN/m was obtained at the interface of crude oil and the emulsion. A favorable wettability alteration of rock from intermediate-wet to water-wet was revealed by contact angle measurement and an enhanced emulsification behavior with crude oil by miscibility test. A tertiary recovery of 21.03% of Original Oil In Place (OOIP) was obtained on sandstone core by optimized emulsion injection. Therefore, performance assessment of optimized emulsion under reservoir conditions confirms its capability as an effective oil-displacing agent.

1 Introduction

The oil and gas industry still being an emerging sector requires an uplift to address the global energy crises. The crude oil present in rock pores usually extracted by conventional methods *i.e.*, primary and secondary recovery leaves about two thirds of Original Oil In Place (OOIP) in the reservoir that cannot be recovered. The introduction of Enhanced Oil Recovery (EOR) techniques or tertiary recovery using chemical blends (chemical-EOR) with mechanism of Interfacial Tension (IFT) reduction, wettability alteration and mobility ratio improvement at this stage have been widely used (Pal *et al.*, 2018; Pei *et al.*, 2012). The uncertain behavior of *in-situ* emulsions, loss of costly tailor made chemicals or surfactant on rocks surfaces make chemical-EOR un-economical (Zhang *et al.*, 2011). Therefore, to transform the current situation of oil production advancement of an improved EOR strategy is obligatory. Employment of surfactant based emulsions in EOR can be a revolution if properly applied. An emulsion is a system of two immiscible fluids basically oil and water usually stabilized by a surfactant, in which one phase gets dispersed in the other (Binks, 1998). Surfactants reduce the IFT at oil-water interface by forming a protective film over the oil droplets which prevents their coalescence by electrostatic repulsion with improvement in continuous phase viscosity (Jafari *et al.*, 2008; Kumar and Mandal, 2020). Surfactant stabilized emulsion implementation in enhancing oil recovery has prior been accounted in earlier studies (Egbogah and Dawe, 1981; Kumar and Mandal, 2018b). During oil recovery emulsion acts by three mechanisms: IFT reduction, alteration of rock surface wettability and trapped

* Corresponding author: ajay@iitism.ac.in

crude oil miscibility (Farouq-Ali, 1976). A reservoir behavior may vary from place to place due to variation in its subsurface condition such as change in formation fluid composition, alkaline or acidic nature, pressure and temperature variation with depth (Allen, 1968; Terry and Rogers, 2014). The stability of an emulsion is referred to its ability to resist change in its behavior with influence of external factors. When injected into the reservoir emulsion encounters with the subsurface conditions that influence its behavior. Researchers have either investigated the effect of ionic strength, pH or varying temperature (Gäbler *et al.*, 2006; Yuan *et al.*, 2015). In the studies carried out, none of them discussed the simultaneous interactions of the subsurface parameters on emulsion properties. The subsurface conditions are very critical in controlling the physiochemical characteristics of an emulsion such as droplet size, stability, viscosity, wettability alteration ability, etc. Hence, subsurface conditions need to be properly optimized to achieve an emulsion with desired characteristics suitable for enhancing oil recovery. The conventional optimization technique which uses One-Factor-At-A-Time (OFAT) strategy needs conduction of large number of experiments which is usually time consuming and often fails to project the desired output (Bezerra *et al.*, 2008). Thus for identification and control of critical parameters experimental design approach offers better choice over OFAT as it handles multivariate data and fits them through an numerical function (Hibbert, 2012). Taguchi Orthogonal Array (TOA) design, which with quite less experiments recognizes the influence of main parameters, is being widely applied in industries because of its robust technique for optimization of parameters (Aggarwal *et al.*, 2008). TOA uses set of special arrays that provide maximum information regarding the influence of involved parameters with minimum experiments. The effects of parameters can be linear, quadratic or of higher orders (Montgomery, 2013).

An emulsion can be prepared by homogenizing two immiscible liquids stabilized by an emulsifier. Surfactant stabilized emulsions with their unique properties have applications in wide sectors *e.g.* cosmetics, pharmaceutical, paint industries (Kang *et al.*, 2002; Karthikeyan *et al.*, 2012). Emulsions may also be applicable in oil fields in fracturing, well bore cleaning, etc. when injected into the reservoir (Amanullah and Al-Tahini, 2009). A stable emulsion formation requires an emulsifier with proper Hydrophilic–Lipophilic Balance (HLB) value. Reduction in IFT with lessening of interfacial energy at oil-water interface by surfactants mobilizes the oil in the reservoir by reducing the capillary forces (Sakthivel *et al.*, 2015). As such stability of emulsion depends upon its droplet size and rheological behavior which are influenced by the type of surfactant used, salinity level (ionic strength), nature of continuous phase *i.e.* acidic or basic (variation in pH) and surrounding temperature. Therefore, droplet size evaluation by Dynamic Light Scattering (DLS) is vital for interfacial nature and stability understanding of an emulsion (Kumar and Mandal, 2018a). For careful examination of emulsion droplets microstructure and its imaging, optical microscopy is the simplest method. The emulsion stability is optimum at a précised value of pH, temperature and ionic strength. A competition between the electrostatic repulsive force and the attracting van der Waals force control the behavior of an emulsion system. The balance between these forces govern the emulsion stability and interfacial assemblage (Ohshima and Makino, 2014). Zeta (ζ) potential investigates the effect of ionic strength at the oil-water interface. Mobility ratio improvement of the displacing fluid by emulsion injection due to viscosity improvement increases the areal sweep efficiency (Clifford and Sorbie, 1985). Shear thinning behavior of emulsion with shear rate lowers the displacing fluid viscosity that improves its injectivity around the injection well (Dong *et al.*, 2008). Fluids under deformation showing viscous and elastic nature and informing about dynamic moduli *i.e.*, viscous/loss modulus (G') and elastic/storage (G'') modulus are known as viscoelastic fluids (Kumar *et al.*, 2017). Wettability is adhesion of a fluid to a solid surface in presence of another immiscible fluid. The adhering fluid on solid surface (such sandstone, dolomite or limestone) is termed as wetting fluid. Wettability denotes the fluid and solid surface interactions, effects the oil recovery rate and the saturation of residual oil (Tiab and Donaldson, 2004). Depending upon the interactions between rock surface and injected slug a system wettability may vary from oil-wet to water-wet (Amirpour *et al.*, 2015). Surfactants modify the wettability by surface tension reduction and by change of interfacial energy between solid-aqueous phases that leads to contact angle variation in solid-aqueous phase-air system. To study the wetting property of emulsion on rock surface wettability alteration was investigated by contact angle measurements. Miscibility and solubilization study evaluates emulsifying behavior, solubilization ratio of oil and aqueous phase and comparative volumes of different phases obtained (Kumar and Mandal, 2018c). IFT calculation at interfaces by theoretical expression is given by Chun-Huh equation (Kanan *et al.*, 2017).

The objective of the present study is to formulate an optimized emulsion using the optimum values of salinity, pH and temperature obtained by analyzing their influence on the properties of surfactant stabilized emulsion with the help of TOA design that can further be applied for industrial applications, such as for enhanced oil recovery. Emulsion was synthesized using *n*-heptane, Sodium Dodecyl Sulfate (SDS) an anionic surfactant and distilled water. SDS, an alkyl sulfate group surfactant was selected because of its ability to considerably reduce the IFT, has high cloud point over 100 °C making it effective at high temperature and the high HLB = 40 value suggests formation of O/W emulsion (Griffin, 1949; Karnanda *et al.*, 2013). The organic solvent (*n*-heptane) was selected as an oleic phase for emulsion preparation because: (a) *n*-heptane is a seven-carbon aliphatic compound which is a natural constituent in crude oil and resembles to lighter crude oil (b) it has a solubility of 3.4 mg/L in water. *n*-heptane adsorbs to suspended solids and sediment when mixed in water thereby enhances the surfactant carrying capacity (c) water-n-heptane interfacial tension measured at 25 °C is lowest compared to other hydrocarbons (Jiao and Burgess, 2003) and (d) n-heptane is biodegradable and is generally considered to be less toxic than other hydrocarbons. Prepared emulsion was evaluated

by droplet size, ζ-potential, conductivity, bottle testing, contact angle measurement, miscibility property and fluid nature by rheological behavior analysis for elucidating emulsion potency in enhancing oil recovery. To test the functionality of the formed optimized emulsion in enhanced oil recovery and to compare its efficiency to that of polymer solution, flooding experiments were performed on sandstone core.

2 Experimental section

2.1 Material required

Anionic surfactant Sodium Dodecyl Sulfate (SDS, $NaC_{12}H_{25}SO_4$) having Critical Micelle Concentration (cmc) value of 8.2 mM at 25 °C with HLB value of 40 was purchased from *Emplura, Merck*. *n*-heptane, the oil phase in emulsion was bought from *SRL Chemicals*. Sodium chloride (NaCl, purity > 99%), hydrochloric acid (HCl) and NaOH pellets used for pH variation were procured from *Rankem Chemicals*. Polymer, Pusher 100 (Partially hydrolyzed polyacrylamide, PHPA – a water soluble polymer with density 850–950 kg/m^3) was acquired from *M/S SNF Floerger, SNF SAS*, ZAC de Millieux, Andrézieux, France. The aqueous polymer solution with 1.5 wt.% of PHPA was prepared as per API RP 63 (*American Petroleum Institute*: Recommended Practices for evaluation of polymers used in EOR operations). All chemicals were used as obtained without further purification. For miscibility test and core flooding experiments crude oil was obtained from *ONGC*, India. Double distilled water (*Millipore SA*, 67120 Molsheim, France) was used in all solution preparations.

2.2 Emulsion preparation

O/W emulsions (confirmed from the conductivity values) were prepared in constant ratio 9:1 (wt.%) of aqueous SDS solution and *n*-heptane. Firstly, aqueous SDS solution was prepared by proper mixing of SDS (concentration taken 10% higher than its cmc, *i.e.*, 110% of cmc in view of surfactant requirement in emulsion droplet stability) and double distilled water with the help of magnetic stirrer at 400 rpm for 10 min. Secondly, *n*-heptane was gently poured into the aqueous SDS solution with continuous stirring for 1 h to form a homogeneous mixture or emulsion. Prepared emulsions were subjected to further characterization with individual and combined effect of salinity, pH and temperature.

2.3 Experimental design and optimization

A well planned experimental design with set of experiments having all interest parameters over specified range is a better approach to acquire desired systematic results. Present study uses Taguchi method (statistical method) based on Orthogonal Array (OA) for design of experiments using Design expert 7.0.0. A minimum (well-defined) set of experiments is provided by OA which provides much reduced variance in experiments, thus saves time and makes it more efficient. In addition, Analysis Of Variance (ANOVA) was employed for statistical analysis of response data to better understand parameter – response relation using quadratic model. Three operating variables namely salinity, pH and temperature were considered and a suitable orthogonal array was selected accordingly followed with conducting of experiments. A Taguchi four level approach with 16 runs was used to show the influence of variables on responses. Table 1 presents variables and their levels. After optimization of variables as per obtained response an optimized emulsion was formulated for characterization to be applied in enhanced oil recovery.

Table 1. Independent variables values used in Taguchi experimental design.

Factors	Unit	Levels			
		1	2	3	4
A: Salinity	wt.%	0.1	0.5	1.0	2.0
B: pH		3.0	5.0	8.0	10.0
C: Temperature	°C	30	40	50	60

2.4 Salinity and pH variation

Emulsion formulation was followed by NaCl addition and pH variation as obtained the combinations of NaCl concentrations, pH and temperature variations from the experimental design. NaCl was added in different amounts (0.1, 0.5, 1.0 and 2.0 wt.%) with stirring for 5 min. Accordingly pH of emulsions was adjusted to its preferred values (3.0, 5.0, 8.0 and 10.0) with the formulated buffer solutions (0.1 N of HCl for acidic behavior and 0.1 N NaOH for basic behavior). The pH of prepared O/W emulsions after NaCl addition was measured by directly immersing the electrode into the emulsions using a digital pH meter (model – 111, EI) calibrated using standard solutions of known pH (4.0, 7.0 and 9.0) at 25 °C ± 1 °C. pH readings from the instrument were precisely read with measurement done in triplicate.

2.5 Physicochemical properties evaluation

2.5.1 Screening of emulsions

Prepared emulsions after NaCl addition and pH adjustment were characterized for their droplet size, surface charge (zeta potential), conductivity and viscosity property at required temperatures for formulation of an optimized emulsion.

Emulsion droplet size, surface charge and conductivity measurement

Droplet size, zeta potential and conductivity were measured by Zetasizer Nano-ZS (*Malvern Instruments*, UK). To avoid multiple scattering due to the viscosity effect caused because of emulsion compositions, emulsions were diluted in the ratio 1:10 in double distilled water before measurement. Zeta potential measurement gives the surface charge (electrical charge) value on the emulsion droplets (positive/negative) in millivolts (mV). The average value of two

separate Zeta potential measurements are reported in the study. Conductivity values correspond for the type of emulsion formed i.e., weather Oil-in-Water (O/W) or Water-in-Oil (W/O).

Viscosity determination

Emulsions viscosity was measured by Bohlin Gemini-2 rheometer, Germany using cup and bob geometry. Flow geometries were obtained in 0.1–500 s^{-1} shear rate. Rheological behavior of the emulsion was described by Power law model (Eq. (1)):

$$\mu = k \times \dot{\gamma}^{n-1}, \quad (1)$$

where, μ apparent viscosity (Pa s), k is the consistency index (dimensionless), $\dot{\gamma}$ is the shear rate (s^{-1}) and n is the flow behavior index (dimensionless). Analysis of droplet size, surface charge, conductivity and viscosity values account for the stability of emulsions.

2.5.2 Optimized emulsion characterization

Addition to droplet size, conductivity, zeta potential and viscosity, formed optimized emulsion was also characterized in terms of its viscoelastic nature, wetting property (contact angle), stability by bottle testing, miscibility and interfacial behavior with microscopic imaging.

Viscoelastic behavior investigation

Viscoelastic behavior investigation informs about the viscous and elastic nature of a fluid. A viscoelastic fluid has partial viscous and partial elastic behavior at changing strain. As a function of angular frequency (ω) the measurements of dynamic moduli *i.e.*, viscous/loss/imaginary modulus (G'') and elastic/storage/real modulus (G') is possible in a viscoelastic fluid. G'' and G' moduli were measured by oscillatory mode and their curves were plotted with varying angular frequency at two different temperatures (30 °C and 70 °C). Fluid shows a viscous nature when $G' < G''$ and a solid like nature when $G' > G''$.

Wetting nature

A flat quartz rock sample of dimension 20 × 20 × 5 mm cut using trimming machine and polished by polishing tools to minimize surface roughness was properly cleaned by acetone and double distilled water following vacuum drying to remove adsorbed contaminants. For proper aging the vacuum dried quartz specimen was dipped in crude oil for 60 days at 323 K. The wettability nature changed to intermediate wet. A Drop Shape Analyzer (*Kruss DSA25*, Germany) was used to measure the dynamic contact angle using sessile drop method by dropping a volume of 2 µL of optimized emulsion on the quartz specimen surface. To maintain the surrounding temperature the oil aged quartz specimen was positioned in a temperature-humidity compartment. Restoration of temperature-humidity compartment to its internal humidity was allowed after every measurement. For every measurement a new area of rock surface was selected to avoid contamination from emulsion traces.

Hydrolytic stability, miscibility study, interfacial tension and microscopic imaging

Optimized emulsion stability was analyzed by bottle test method. Emulsion was stored in an air tight 15 mL glass tube at 70 °C. Miscibility test at desired pH and salinity with crude oil was performed by mixing optimized emulsion and crude oil for 2 h with the help of Rivotek horizontal shaker in the ratio 1:1 (5 mL each in glass tube). The extent of crude oil miscibility in emulsion is indication of better oil recovery which in turn depends on the mixing time of the fluids. To represent the reservoir temperature condition glass tubes (of stability and miscibility tests) were kept in an oven at a constant temperature of 70 °C. Separation of different fluid phases in stability and miscibility tests was optically observed with the help of high definition camera (Nikon Coolpix L-840) at stipulated time. The interfacial activity of optimized emulsion with crude oil was investigated by determination of interfacial tension value. The IFT values at crude oil-middle emulsion and water-middle emulsion were calculated by Chun-Huh equation (Eq. (2)):

$$\sigma_{\mathrm{om}} = \frac{c}{\left(\frac{V_{os}}{\mathrm{Vs}}\right)^2}; \ \sigma_{\mathrm{wm}} = \frac{c}{\left(\frac{V_{ws}}{\mathrm{Vs}}\right)^2}, \quad (2)$$

where, c is a constant ($c = 0.3$ mN/m) which is consistent for this type of systems, σ_{om} and σ_{wm} are the IFT between crude oil-middle emulsion and water-middle emulsion respectively. $\left(\frac{V_{os}}{\mathrm{Vs}}\right)$ and $\left(\frac{V_{ws}}{\mathrm{Vs}}\right)$ are the ratios of volume of oil and water solubilized in total volume of surfactant respectively. A detailed explanation of solubilization parameters calculations with their equations can be found in our previous work (Kumar and Mandal, 2018c). The morphology of droplets of optimized emulsion was captured with the aid of a high resolution optical microscope (Olympus BX51) equipped with Stream Basic 2.1 image analysis software.

2.5.3 Oil recovery experiment

To test the oil recovery efficiency of the optimized emulsion and to compare it with aqueous polymer solution flooding experiments were carried out on a sandstone core of length 7.7 cm and diameter 3.8 cm at 70 °C. Prior to each flooding experiment sandstone core was cleaned with distilled water, then washed by methanol-toluene mixture (1:1) followed by drying in an oven. The sandstone core was saturated with 1% NaCl brine for 24 h period allowing its complete saturation. Porosity was determined by weight measurement of the sandstone core before and after brine saturation. The sandstone core was placed in the core-holder with a confining pressure of ~1000 psi. Thereafter, flooding the sandstone core with brine for absolute permeability determination (k). The absolute permeability of the sandstone core was calculated using Darcy equation: $q = \frac{kAdp}{\mu dx}$, where k is permeability in Darcy, μ is the fluid viscosity (cp), A is the cross sectional area of the sandstone core (cm^2) and dp/dx is the pressure gradient (atm/cm). The sandstone core was flooded with crude oil to irreducible water saturation (S_{wi}) after brine saturation and left for 7 days for the effective oil wetting. Then water flooding or secondary

Table 2. Design of experiments with independent variables and their corresponding responses.

Run	Salinity (A)	pH (B)	Temperature (C)	Responses				
				Droplet size (nm)	Zeta potential (mV)	Conductivity (mS/cm)	n	k
1	1.00	10.00	40.00	2417.94	−48.4	21.4	0.544	0.009
2	1.00	3.00	50.00	2503.58	−37.4	22.2	0.565	0.014
3	0.50	5.00	30.00	2563.38	−54.3	12.1	0.613	0.009
4	0.10	3.00	30.00	2761.87	−82.7	2.66	0.579	0.011
5	1.00	8.00	30.00	2831.51	−49.2	20.7	0.582	0.009
6	0.50	10.00	50.00	2976.25	−50.9	13.1	0.573	0.011
7	0.10	10.00	60.00	2996.92	−59.4	3.0	0.544	0.014
8	2.00	3.00	60.00	3351.14	−7.55	44.6	0.599	0.012
9	0.10	5.00	40.00	3451.80	−70.4	3.06	0.501	0.011
10	2.00	8.00	40.00	3695.02	−13.9	42.2	0.564	0.011
11	0.10	8.00	50.00	3506.32	−62.3	3.49	0.588	0.01
12	0.50	3.00	40.00	2460.81	−58.3	11.78	0.495	0.015
13	0.50	8.00	60.00	3658.18	−45.6	12.35	0.609	0.008
14	1.00	5.00	60.00	3795.19	−33.4	23.06	0.583	0.011
15	2.00	10.00	30.00	4677.30	−31.3	41.91	0.564	0.014
16	2.00	5.00	50.00	3035.88	−3.5	43.41	0.577	0.01

recovery was performed followed by chemical slug (optimized emulsion or aqueous polymer solution) injection. Lastly, chase water flooding with brine solution of 1.0 wt.% NaCl was done.

3 Results and Discussion

3.1 Experimental design

The proposed experimental design suggested by Taguchi method with independent variables (A: salinity, B: pH and C: temperature) and their response on emulsion characteristics (droplet size, surface charge, conductivity and viscosity parameters) are presented in Table 2. A set of total 16 experiments (Run) were suggested with objective to obtain best possible response for emulsion characteristics on interactions of different variables. The analysis of responses (16 each) by Taguchi OA followed polynomial behavior with quadratic model except for "n" which followed mean model as their base for Analysis Of Variance (ANOVA). With the attainment of significant experimental model, further studies on the effect of variables on nature of emulsion were carried out, after the fitness of model was tested. The fitness of experimental model was tested by ANOVA with analysis of notable effect of variables interactions on emulsion properties. F-value (Fisher's F-test value) and p-value indicate the impact of variables on responses with accuracy of model. F-value, the ratio of mean square of model to that of residual error approves the statistical significance and prominence of the model. The high F-value and low p-value denote the significance of model with apparent influence of independent variables on responses. Further, the influence of variables at an explicit point over the range were assessed by perturbation curve. A perturbation curve helps in comparing the influence of different variables in the designed space at a particular point. For two or more variables perturbation plot is beneficial as it finds those variables that most affect the response. The response is analyzed by varying only one variable in its range while other variables remain constant. A curvature or incline in variable indicates the sensitiveness of response to that variable or else insensitiveness to that variable with a straight line or flat curve. Additionally, three dimensional (3-D) surfaces were plotted to get a better insight about the interaction effect of independent variables on responses. The individual and combined influence of independent variables on emulsion properties are studied in further sections.

3.2 Response to independent variables

Obtained results were statistically analyzed to identify the significant terms based on interactions of variables. Individual and combined response of independent variables are presented in the study. Most important or significant variable would be based on their F-value and p-value as obtained from ANOVA analysis.

3.2.1 Conductivity

The ANOVA for conductivity response suggested a quadratic model. Table 3 illustrates ANOVA for conductivity response. As observed, the model with F-value of 117.08 implies the model is significant and with p-values less than 0.05 (95% confidence level) indicate model terms are significant. In conductivity response A and A^2 are significant model terms, inferring that salinity has the most influence on conductivity. The conductivity response in terms of

Table 3. ANOVA analysis for conductivity response.

Source	Sum of Squares	Degree of Freedom	Mean Square	*F*-value	*p*-value	
Model	48.89	9	5.43	117.08	< 0.0001	Significant
A-Salinity	16.96	1	16.96	365.54	< 0.0001	
B-pH	0.0007	1	0.0007	0.0160	0.9034	
C-Temp.	0.0169	1	0.0169	0.3650	0.5679	
AB	1.151E-06	1	1.151E-06	0.0000	0.9962	
AC	0.0029	1	0.0029	0.0631	0.8100	
BC	0.0071	1	0.0071	0.1534	0.7089	
A^2	1.46	1	1.46	31.52	0.0014	
B^2	0.0013	1	0.0013	0.0273	0.8742	
C^2	0.0034	1	0.0034	0.0724	0.7969	
Residual	0.2784	6	0.0464			
Cor total	49.17	15				

independent variables in quadratic equation form is presented as below (Eq. (3)):

$$\begin{aligned}\text{Sqrt (Conductivity)} = {} & +1.23446 + 4.14529 \times A \\ & - 0.026002 \times B + 0.007676 \\ & \times C - 0.000281 \times A \times B \\ & + 0.003420 \times A \times C \\ & + 0.001217 \times B \times C \\ & - 0.846369 \times A^2 \\ & - 0.001780 \times B^2 \\ & - 0.000145 \times C^2 \end{aligned} \quad (3)$$

where, A is salinity in wt.%, B is the pH and C denotes the temperature in °C. A positive (+) or negative (−) sign in front of a term indicates the synergistic or antagonistic effect respectively. From ANOVA Table 3, pH has negligible impact on conductivity values with low F-values and high p-values, whereas temperature effects conductivity values but is of not much significant as salinity. The perturbation plot (Fig. 1) also indicates the importance of salinity in comparison to pH and temperature. Therefore, effect of salinity and temperature on conductivity is only explained. At constant temperature (say for 30 °C) conductivity values raised from 2.66 mS/cm to 41.91 mS/cm with increase in salinity from 0.1 wt.% to 2.0 wt.% (Tab. 2). The physical reason to such behavior can be explained as following. Pure water (continuous phase) does not conduct electricity as there are no ions present it. When NaCl is diffused into pure water NaCl breaks into Na^+ and Cl^- ions that conduct electricity on application of potential difference. This behavior can also be explained in term of conductance (G), which depends upon the geometry (M) (shape and size) of ions. In an ionic compound, usually entire ions diffuse to conduct electricity on application of potential difference as discussed above. The diffused ions are less mobile due to large size as compared to electrons depending on potential difference, temperature and their geometry (smaller the ion more rapid is the movement). In continuous phase (water) hydrogen (H^+) and hydroxyl (OH^-) ions are extremely mobile because of their smaller size as compared to Na^+ and Cl^- ions in aqueous solution or in emulsions. As conductance is directly proportional to the size of ions *i.e.* $G \propto M$. The conductivity in presence of Na^+ and Cl^- ions will be higher than that for hydrogen (H^+) and hydroxyl (OH^-) ions and it will increase with rise in salinity (Golnabi *et al.*, 2009; Xu *et al.*, 2015). Also, the increase in NaCl concentration is an indication of increase in emulsification behavior because of the enhanced activity of surfactant molecules present at oil-water interface due to accumulation of NaCl (Na^+ and Cl^- ions) at the surfactant molecules surface which helps in Interfacial Tension (IFT) reduction at oil drops (Leong *et al.*, 2009). In general, conductivity of colloidal suspension increases with temperature. At constant

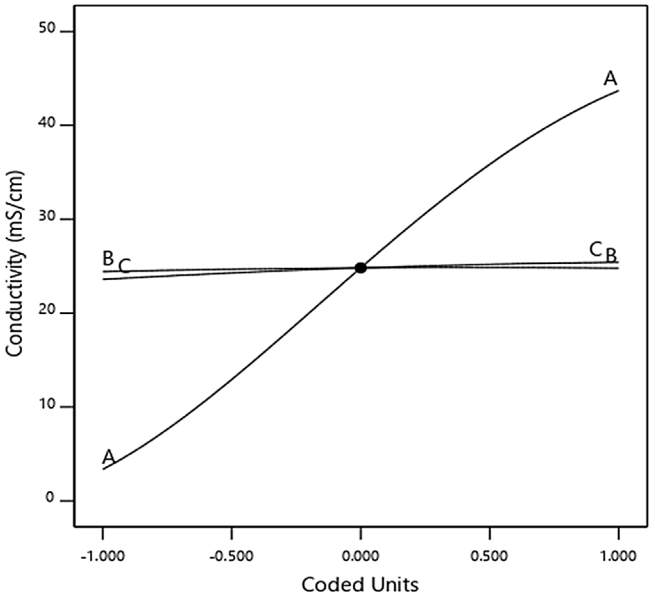

Fig. 1. Perturbation curve of conductivity response with different factors, A: salinity, B: pH and C: temperature.

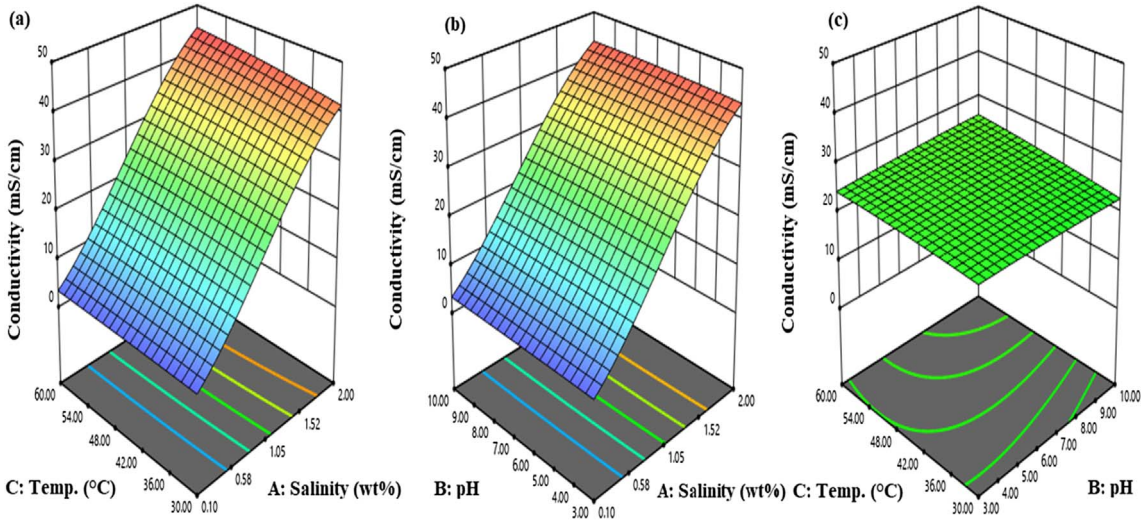

Fig. 2. 3-D curve for conductivity response as a function of the three independent variables.

salinity (say 1.0 wt.%) there is rise in conductivity value from 20.7 mS/cm to 23.06 mS/cm with increase in temperature from 30 °C to 60 °C. This behavior is due to the enhanced mobility of oil droplets in the continuous medium with rise in temperature. The increased oil droplets mobility in continuous phase leads to their simultaneous breakdown and re-coalescence, which is a process of emulsion formation (Allouche *et al.*, 2004). Moreover rise in temperature increases the interfacial area at oil-water interface which in turn helps in IFT reduction, hence favors oil emulsification. To gain more insight about the combined effect of independent variables on conductivity response 3-D surfaces were plotted. Figure 2 presents the 3-D conductivity plot as a function of salinity-temperature (AC), salinity-pH (AB) and pH-temperature (BC). In Figures 2a and 2b there is an increase in conductivity with variation of AC and AB being pH and temperature constant respectively, as also evident from the ANOVA Table 3. There is not much variation observed in Figure 2c with variation of BC, as the significant factor A (salinity) is kept constant. The conductivity values as observed from Table 2 being higher than 2 mS/cm favor the formation of Oil-in-Water (O/W) emulsion (Huang *et al.*, 2001) for each 16 combinations which is a desired output at reservoir condition for oil recovery.

3.2.2 Droplet size

In emulsions, droplet size distribution can be a determining factor for their stability irrespective of coalescence of oil droplets (McClements, 2004). The droplets size in O/W emulsions depends upon salinity, pH and temperature. The ANOVA analysis for droplet size response suggested a quadratic model as for conductivity response. The ANOVA for droplet size response is presented in Table 4. With F-value of 13.03 the model is significant and with p-value of 0.0027 (< 0.05 *i.e.*, 95% confidence level) shows the model terms are significant. In droplet size response C, AB, BC, A^2, B^2 and C^2 are significant model terms, deducing that droplet size is effected by all the three variables rather than only single variable as in the case of conductivity response. The terms A^2, B^2 and C^2 simply are the square terms of the independent variables A, B and C for the response on the droplet size, as obtained from the quadratic equation. The square of a term is not related to its concentration. The influence of the term (trend) will be the same irrespective of its square. The perturbation plot for droplet size response is shown in Figure 3. The quadratic equation form for droplet size response in terms of independent variables is shown as below (Eq. (4)):

$$\begin{aligned}\text{Droplet size} = {} & 1266.27375 - 3309.71271 \times A \\ & + 780.83467 \times B - 21.26692 \times C \\ & + 248.00389 \times A \times B - 4.20201 \\ & \times A \times C - 12.31409 \times B \times C \\ & + 825.25651 \times A^2 - 29.89343 \times B^2 \\ & + 1.61744 \times C^2 \end{aligned} \quad (4)$$

where, variables A, B and C with (+) and (−) signs are same as discussed in the above section. As per ANOVA Table 4, temperature (C) with F-value of 15.57 and p-value of 0.00076 has the most impact on droplet size with less of pH (F-value of 5.52 and p-value of 0.0571) and salinity (F-value of 1.38 and p-value of 0.2850). At constant salinity (say 0.1 wt.%), with increase of temperature and pH from 30 °C to 50 °C and 3 to 8 respectively there is rise in droplet size from 2761.87 nm to 3506.32 nm (Tab. 2). In an emulsion the oil droplets are coated with surfactant layer, in this case of SDS which creates an electrostatic barrier that prevents their coalescence (Pal *et al.*, 2019a). If we discuss the effect of temperature (C) on the droplet size, the electrostatic barrier gets loosen up with rise in temperature that promotes the coalescence of oil droplets, thus increase in droplet size. In general, with increase in temperature a drop in pH is observed that screens out the electrostatic barrier helping in coalescence of oil droplets. Since in the study a simultaneous increase

Table 4. ANOVA analysis for droplet size response.

Source	Sum of squares	Degree of freedom	Mean square	*F*-value	*p*-value	
Model	5.374E+06	9	5.971E+05	13.03	0.0027	Significant
A-Salinity	63130.78	1	63130.78	1.38	0.2850	
B-pH	2.529E+05	1	2.529E+05	5.52	0.0571	
C-Temp.	7.137E+05	1	7.137E+05	15.57	0.0076	
AB	8.936E+05	1	8.936E+05	19.50	0.0045	
AC	4423.03	1	4423.03	0.0965	0.7666	
BC	7.283E+05	1	7.283E+05	15.89	0.0072	
A^2	1.391E+06	1	1.391E+06	30.34	0.0015	
B^2	3.574E+05	1	3.574E+05	7.80	0.0315	
C^2	4.186E+05	1	4.186E+05	9.13	0.0233	
Residual	2.750E+05	6	45833.04			
Cor Total	5.649E+06	15				

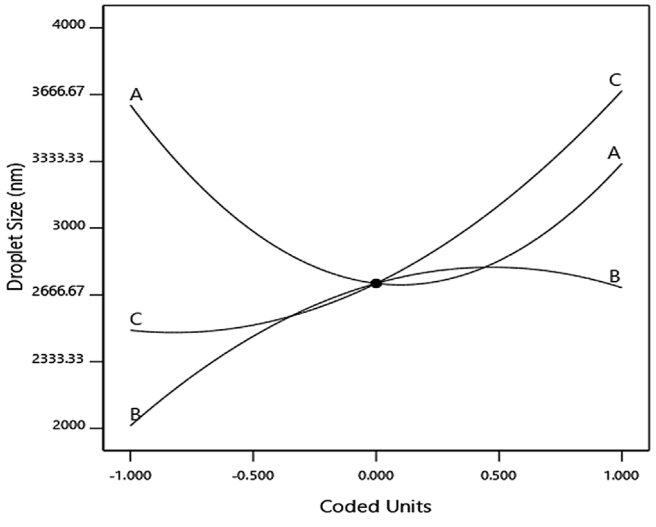

Fig. 3. Perturbation curve of droplet size response with different factors, *A*: salinity, *B*: pH and *C*: temperature.

in pH of emulsion is maintained that helps in stabilization of the barrier, but the increase in droplet size till 50 °C indicates the dominance of temperature over pH (till pH value 8). With further temperature increase to 60 °C drop in droplet size indicates the dominance of pH (>8) suggesting stabilization of the barrier that prevents the destabilizing effect of temperature (interaction of *BC*). The reason to this behavior can be explained as following. A series of complex phenomenon occurs simultaneously. With temperature rise weakening of electrostatic barrier and increase in vibrational energy of oil droplets takes place due to which their breakdown and re-coalescence occur. The slow surfactant layer formation or electrostatic barrier around the newly formed oil droplets during breakdown leads the dominance of re-coalescence process. The simultaneous increase of pH (*B*) with temperature helps in prevention of coalescence of oil droplets due to accumulation of large number of OH^- ions in the continuous phase that repels the newly formed negatively charged SDS surfactant coated oil droplets, hence prevent their coalescence. The dominance of temperature overcomes the pH effect up to 50 °C due to which coalescence of oil droplets occurs, hence increase in their size. Further temperature rise (60 °C) only enhances the vibrational energy leading to breakdown of oil droplets rather than their coalescence because of the dominance of pH effect. The ions influence the interactions between oil droplets in so many ways that it is very difficult to accurately quantify their effect on emulsion behavior. As such salt addition to a suspension alters its physiochemical properties (salinity effect, *A*). It's been earlier reported that addition of salt leads to increase in oil droplet size as it induces the thinning of the Electric Double Layer (EDL) because of the electrostatic screening effect of salt (Park *et al.*, 2018). The EDL prevents the coalescence of oil droplets by electrostatic repulsion, by its thinning oil droplets tend to combine. At salt concentration above a particular limit the electrostatic barrier is no longer sufficiently strong to overcome the attracting forces *i.e.* van der Waals attractions (Hunter, 1998). At constant temperature (say 30 °C) an increase in droplet size is observed with addition of salt, with an exception at low salinity (Tab. 2). The droplet size decreased from 2761.87 nm to 2563.38 nm when salinity and pH increased from 0.1 wt.% to 0.5 wt.% and 3 to 5 respectively. The drop in droplet size with salinity increase is due to the enhanced accumulation of Na^+ ions at the surface of oil droplets causing reduction in interfacial tension leading to formation of elongated worm like micelles with smaller diameter from spherical micelles (oil droplets). Also drop in droplet size shows the dominance of pH effect over salinity effect at low salt concentration. With further increase of salinity from 0.5 wt.% to 2.0 wt.% an increase in droplet size was observed as reported in earlier studies. As explained before the electrostatic screening effect of salt at high salinity is the cause of this behavior. Also a surfactant stabilized emulsion is sensitive to the ionic strength which increase at high salt concentrations, ultimately leading to such a behavior (Garti *et al.*, 1999). The dominance of salinity over the increase in pH is

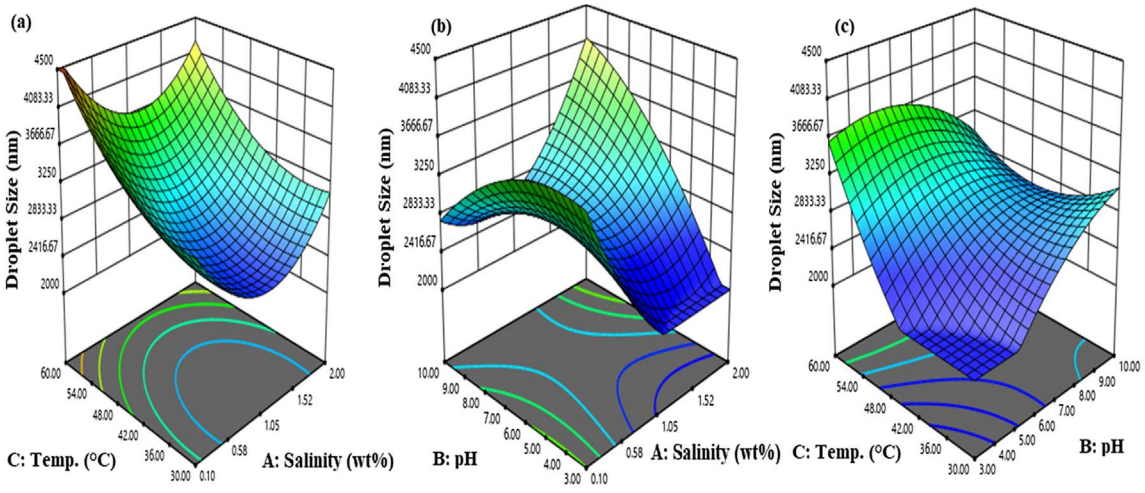

Fig. 4. 3-D plot for droplet size response as a function of the three independent variables.

observed by increase in droplet size (interaction of AB). This can also be verified from the ANOVA Table 4. 3-D plots for droplet size response as a function of AC, AB and BC were plotted for better understanding of their combined interaction, Figures 4a–4c.

3.2.3 Zeta potential

Zeta (ζ) potential provides the surface or electrical charge on oil droplet surface that informs about the behavior of emulsions (Moreira de Morais *et al.*, 2006). Surface charge can both be positive and negative ($\pm$) with a magnitude. An absolute ζ-potential value above $\pm$ 30 mV is an indicative of emulsion stability to aggregation of droplets (Jourdain *et al.*, 2008). A quadratic model for ζ-potential response was suggested by ANOVA analysis. The significance of the model and the model terms are justified by F-value of 109.13 and p-value < 0.001 (< 0.05 *i.e.*, 95% confidence level) respectively as seen from ANOVA Table 5. In ζ-potential response A, AB, BC and B^2 are the significant model terms, inferring that surface charge is influenced by all three independent variables as for the droplet response. As discussed in previous section square of a term just indicates the quadratic form of that term with the same influence. The model equation of ζ-potential response in terms of independent variables in quadratic form is shown as below (Eq. (5)):

$$\begin{aligned}\text{Zeta potential} = {} & -119.16714 + 64.51631 \times A \\ & + 3.84348 \times B + 0.937891 \times C \\ & - 2.19697 \times A \times B - 0.230176 \\ & \times A \times C + 0.097836\, B \times C \\ & - 4.05452 \times A^2 - 0.541875 \times B^2 \\ & - 0.011469 \times C^2, \end{aligned} \quad (5)$$

where, variables A, B and C with (+) and (−) signs are same as discussed in the above sections. As per ANOVA Table 5, salinity (A) with F-value of 352.55 and p-value of <0.0001 influences the ζ-potential the most with less effects of pH (F-value of 4.27 and p-value of 0.0843) and temperature (F-value of 5.43 and p-value of 0.0587). This conclusion can also be drawn from the perturbation plot for ζ-potential response, Figure 5. At constant temperature (say 30 °C), drop in ζ-potential values is observed from −82.7 mV to −31.3 mV with increase in salinity and pH from 0.1 wt.% to 2.0 wt.% and 3–10 respectively (Tab. 2). The decrease of surface charge with rise in salinity (effect of A) is an expected trend and has also been reported in earlier studies (Acedo-Carrillo *et al.*, 2006; Hunter, 1986). This trend can be explained as following. With increase in salinity ionic strength increases that leads to reduction of electrostatic repulsion because of electrostatic screening effect of salt that leads to droplet coalescence which can also be concluded from the increase in droplet size (Harnsilawat *et al.*, 2006). As such ζ-potential is measured by electrophoresis technique in which ζ-potential values are proportional to the mobility of oil droplets under an applied electric field. Thus, the increase in droplet sizes may also be responsible for the reduction in ζ-potential values. As such at first glance a vast influence of pH on ζ-potential values is observed (Tab. 2), but from ANOVA analysis and perturbation curve only a marginal effect can be seen of pH on ζ-potential. The level up to which pH variation causes a change in ζ-potential seems to depend up on salinity (interaction of A and B). A small drop in ζ-potential value with pH is observed at high salinity. This behavior can be explained as following. As discussed the oil droplets are coated with SDS surfactant molecules (SO_4^{2-}) forming an EDL. A rise in ions (Na^+, Cl^-, H^+ and OH^-) concentration with increase in salinity and pH leads to overcrowding of the potential ions at the binding sites available at oil droplet surface *i.e.*, EDL. H^+ ion being reactive to Cl^- and OH^- ion being larger in size leave Na^+ ion as the potent ion to penetrate the EDL and largely effect the ζ-potential values. Therefore, at high salinity only marginal effect on the ζ-potential values is observed for any change in H^+ and OH^- concentration (change in pH). Temperature being an insignificant variable marginally influences ζ-potential. A decrease in

Table 5. ANOVA analysis for zeta potential response.

Source	Sum of squares	Degree of freedom	Mean square	*F*-value	*p*-value	
Model	7319.91	9	813.32	109.13	< 0.0001	Significant
A-Salinity	2627.39	1	2627.39	352.55	< 0.0001	
B-pH	31.83	1	31.83	4.27	0.0843	
C-Temp.	40.44	1	40.44	5.43	0.0587	
AB	70.13	1	70.13	9.41	0.0220	
AC	13.27	1	13.27	1.78	0.2305	
BC	45.97	1	45.97	6.17	0.0476	
A^2	33.57	1	33.57	4.50	0.0780	
B^2	117.45	1	117.45	15.76	0.0074	
C^2	21.05	1	21.05	2.82	0.1439	
Residual	44.71	6	7.45			
Cor Total	7364.63	15				

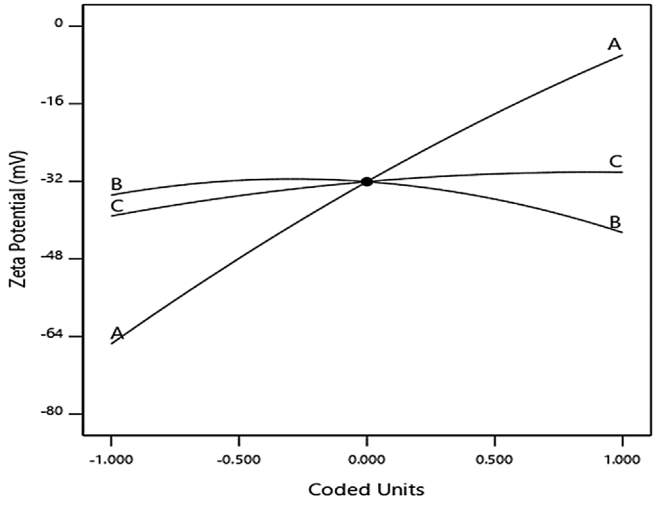

Fig. 5. Perturbation curve of zeta potential with different factors, *A*: salinity, *B*: pH and *C*: temperature.

ζ-potential is seen at constant salinity (say 0.1 wt.%) with change in pH and temperature from 3 to 10 and 30 °C to 60 °C respectively (interaction of *B* and *C*). This drop in ζ-potential can be due to overcrowding of OH^- around EDL because of which an increase in droplet size occurs, thus slow mobility and small ζ-potential values. Though at high temperature (60 °C) a drop in droplet size is observed because of enhanced vibrational energy of droplets leading to their breakage, but the drop in ζ-potential suggests the dominance of pH over temperature. Above deductions can be understood in a better way from the 3-D plots for ζ-potential response as a function of *AC*, *AB* and *BC*, Figures 6a–6c. From the analysis, salinity being the most significant variable dominates over the influences of pH and temperature for ζ-potential response.

3.2.4 Rheological analysis

The rheological analysis of a fluid basically comprises the viscosity study that informs about the fluid flow and its consistency over a shear rate range.

(a) Flow behavior index (n)

The fluid behavior of emulsion that is pseudo-plastic or dilatant nature was studied by its rheological characterization. The emulsion sample was placed in a cup and the shear applied by the rotational motion of the bob determined the required torque for shear stress calculation. Table 2 presents the value of flow behavior index (n) which defines the nature of emulsion, influenced by the three independent variables. If $n = 1 \rightarrow$ Newtonian fluid, $n < 1 \rightarrow$ Pseudo-plastic and $n > 1 \rightarrow$ Dilatant fluid. Since, value of "n" in every case is less than 1 ($n < 1$), the emulsion shows a non-Newtonian or pseudo-plastic behavior (Al-Zahrani and Al-Fariss, 1998). Thus, with an increase in shear rate a drop in apparent viscosity is observed which improves flow ability of emulsion. The disruption of the micellar structure formed by the surfactant molecules in the solution and the alteration in the alignment of emulsion droplets along the flow streamline with increase in shear rate causes the drop in apparent viscosity (Lee, 2011). As seen from Table 2 and ANOVA analysis, Table 6a it can be inferred that "n" as such is not influenced by the independent variables also the model equation of flow behavior (n) response was found as shown below (Eq. (6)):

$$n = +0.567500 \tag{6}$$

The 3-D curve of "n" as function of salinity and pH is presented in Figure 7 which also concludes the above outcome.

(b) Consistency index (k)

The type of fluid flow is provided by the flow behavior index (n) but will the flow be consistent or inconsistent is given by the consistency index (k). ANOVA analysis suggested a quadratic model for consistency index response. With *F*-value of 4.86 and *p*-value of 0.0338 (< 0.05 *i.e.*, 95% confidence level) from ANOVA Table 6b, the significance of the model and the model terms are justified. In this case *B*, *AC*, B^2 are significant model terms implying that pH has the most influence on "k" with less of salinity and temperature. The square term is just the quadratic form of the term with equivalent influence. The model equation

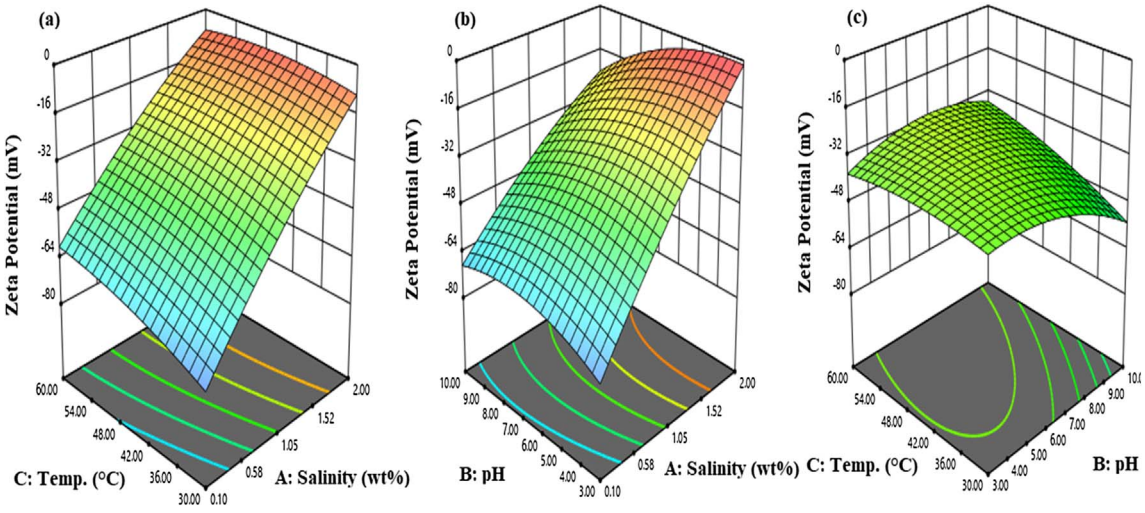

Fig. 6. 3-D curve of ζ-potential response as a function of the three independent variables.

Table 6a. ANOVA analysis for flow behavior response.

Source	Sum of squares	Degree of freedom	Mean square
Model	0.0000	0	
Residual	0.0167	15	0.0011
Cor total	0.0167	15	

of consistency index response in terms of independent variables in quadratic form is shown as below (Eq. (7)):

$$\begin{aligned} k = {} & +0.008244 + 0.011540 \times A - 0.003537 \times B \\ & + 0.000459 \times C - 0.000267 \times A \times B \\ & - 0.000278 \times A \times C - 9.73148\text{E} - 06 \times B \\ & \times C + 0.001217 \times A^2 + 0.000262\, B^2 \\ & - 1.87500\text{E} - 06 \times C^2, \end{aligned} \tag{7}$$

where, variables A, B and C with (+) and (−) signs are same as discussed in the above sections. From ANOVA Tables 6a and 6b, pH (B) with F-value of 13.87 and p-value of 0.0098 influences "k" the most with less of temperature (F-value of 1.42 and p-value of 0.0.2779) and least of salinity (F-value of 0.0549 and p-value of 0.8225). From Table 2, at salinity (say 0.1 wt.%) the value of "k" showed good results at low and high pH values 3 and 10 at 30 °C and 60 °C respectively suggesting an improvement in rheological property, whereas at intermediated pH (5 and 8) a drop in "k" value is observed with 40 °C and 50 °C temperatures (effect of B). This behavior can be attributed to the emulsion droplet size which plays an important role in influences in the rheological property. As observed, emulsion has smaller droplet size at pH 3 and 10 as compared to droplet size at pH 5 and 8. The small emulsion droplets systematically arrange themselves in an ordered way along the flow streamline with improvement in viscosity *i.e.*, maintaining a consistency

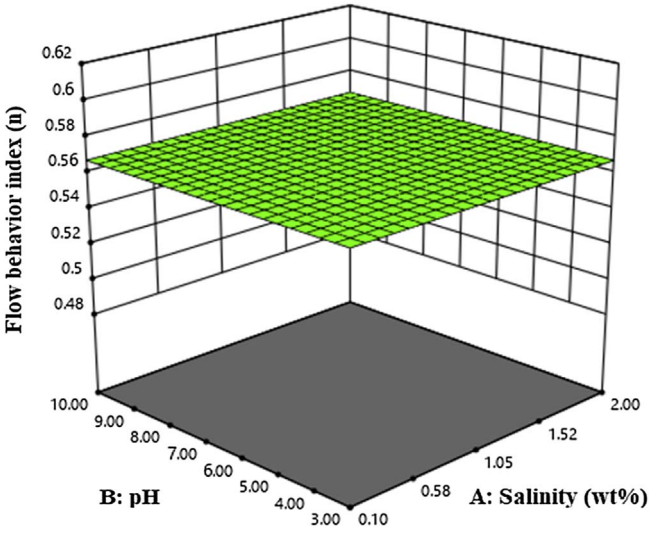

Fig. 7. 3-D curve of emulsion flow behavior (n) as a function of A: Salinity and B: pH.

in viscosity values. The influence of pH and temperature on emulsion droplet size has already been discussed in Section 3.2.2. The consistency of emulsion is also largely influenced by the interaction of salinity and temperature (interaction of A and C). As observed from Table 2 at constant pH (say 3), the value of "k" first increased from 0.011 to 0.015 and then decreased from 0.015 to 0.012 with increase in salinity from 0.1 wt.% to 0.5 wt.% and 0.5 wt.% to 2.0 wt.% with temperature 30 °C and 40 °C and 40 °C and 60 °C respectively. The increase and decrease in value of "k" is due to change in droplet size which is affected by salinity and temperature as discussed in Section 3.2.2. A drop in droplet size favors improvement in consistency of emulsion as discussed above whereas with increase in droplet size leads to distortion in the systematic arrangement of droplets effecting the rheological property. The perturbation curve for

Table 6b. ANOVA analysis for consistency index (k) response.

Source	Sum of squares	Degree of freedom	Mean square	F-value	p-value	
Model	0.0001	9	6.492E-06	4.86	0.0338	Significant
A – Salinity	7.329E-08	1	7.329E-08	0.0549	0.8225	
B – pH	0.0000	1	0.0000	13.87	0.0098	
C – Temp.	1.900E-06	1	1.900E-06	1.42	0.2779	
AB	1.035E-06	1	1.035E-06	0.7753	0.4125	
AC	0.0000	1	0.0000	14.54	0.0088	
BC	4.548E-07	1	4.548E-07	0.3407	0.5807	
A^2	3.026E-06	1	3.026E-06	2.27	0.1829	
B^2	0.0000	1	0.0000	20.65	0.0039	
C^2	5.625E-07	1	5.625E-07	0.4214	0.5403	
Residual	8.010E-06	6	1.335E-06			
Cor total	0.0001	15				

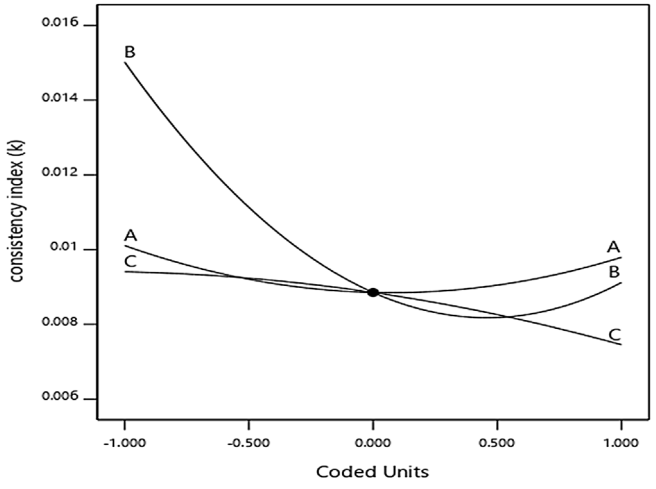

Fig. 8. Perturbation curve of consistency index (k) with different factors, A: salinity, B: pH and C: temperature.

consistency index (k) response shown in Figure 8 also indicates the dominance of pH over salinity and temperature. A large drop in "k" with change in pH is seen as compared to lesser for salinity and temperature. The 3-D plots, Figures 9a–9c present the influence of salinity, pH and temperature on consistency index response.

3.3 Optimization strategy with response verification

To determine the optimum values of the independent variables for desirable response outcome multiple response optimization was carried out. A total of 39 runs were obtained with selection of only the best. For better understanding the variation of the physiochemical properties of emulsion as function of independent variables graphical representations *i.e.*, the 3-D plots are highly recommended (Mason *et al.*, 2003). For overall optimum condition and to determine the exact values of multiple response optimizations graphical visualization was followed by numerical optimization. The best outcome indicated that the emulsion prepared with salinity 0.254 wt.%, pH 3.0 and at temperature 30 °C will provide the ideal region regarding every single physicochemical property contemplated. The desirable response values under the optimum condition for droplet size, zeta potential, conductivity, flow behavior index and consistency index were predicted to be 2417.936 nm, −73.180 mV, 5.642 mS/cm, 0.568 and 0.012 respectively. The verification of the predicted response values obtained from the ideal values of independent variables after optimization was accomplished by comparing them with the obtained experimental values. The experimental response values were obtained by characterizing (in Sect. 3.4) the optimum emulsion formed as per the optimum values obtained for the independent variables. Table 7 presents the comparison of predicted and experimental response values. The experimental response values were in agreement with the predicted values. With no significant difference in predicted and experimental values, the competence of Taguchi OA model is confirmed for analyzing the variation in the physiochemical properties of emulsion as function of salinity, pH and temperature.

3.4 Characterization of optimized emulsion

The formulation of optimized emulsion using the optimum values of salinity, pH and temperature was followed by its characterization for one of the petroleum industry application *i.e.* EOR application. Emulsion was characterized by its droplet size, surface charge, conductivity, hydrolytic stability, wetting (contact angle) and rheological properties with interfacial behavior. Emulsion stability can be directly linked to its droplet size. The presence of surfactant coating over the oil droplets prevents their coalescence, hence improves emulsion stability. For screening of emulsion as injection slug into the reservoir its droplet size evaluation is must. Droplet size should be smaller than the pore throat diameter to prevent its plugging (Harnsilawat *et al.*, 2006). Figure 10a shows the droplet size distribution of the optimum emulsion obtained by dynamic light scattering method. The average droplet size of emulsion was obtained to be 2417.73 nm with a Dispersity Index (DI) of 0.19. DI

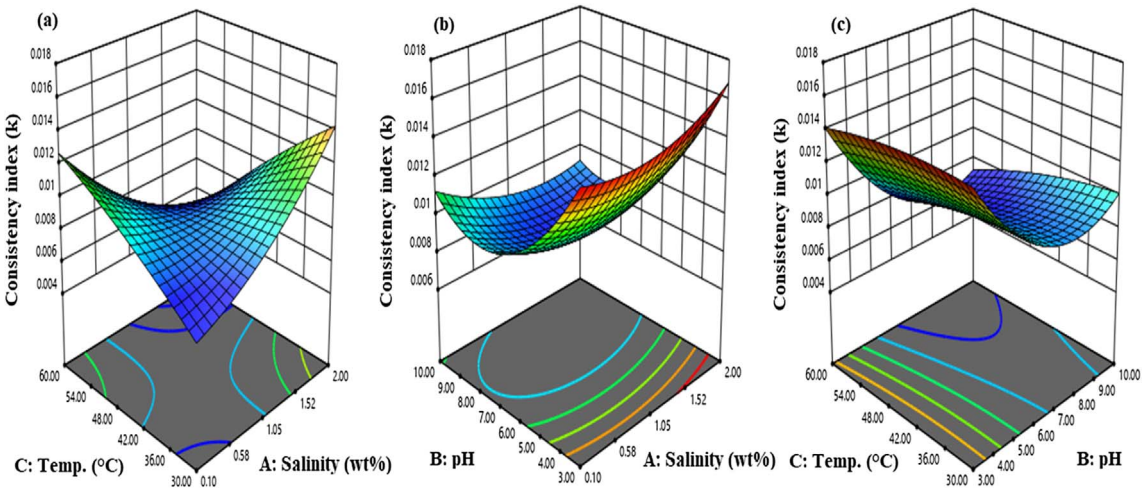

Fig. 9. 3-D curve of consistency index (k) response as a function of the three independent variables.

Table 7. Comparison of predicted and experimental values of response.

Response	Predicted	Experimental	Residue
Droplet size (nm)	2418.47	2417.73	0.74
Zeta potential (mV)	−73.18	−72.52	−0.66
Conductivity (mS/cm)	5.64	5.12	0.52
n	0.56	0.53	0.03
k	0.012	0.020	−0.008

index varies between 0 and 1; 0 for mono-disperse system and 1 for broad distribution. Low DI value suggests good stability of formulated emulsion. Droplet size distribution was examined by Gauss statistical distribution model. With coefficient of determination (R^2) value 0.9788 denotes a good fit of droplet size distribution. The microscopic image depicting the morphology of emulsion droplets of the optimized emulsion is shown in Figure 10b. As observed, emulsion droplets are in good agreement with the droplet size obtained from DLS method. The distribution of droplets shows no sign of coalescence suggesting surfactant layer formation over the oil droplets, thus enhancing the stability of emulsion. For surfactant stabilized emulsion system equilibrium of repulsive (electrostatic) and attractive (van der Waals) force is necessary for stability (Ohshima and Makino, 2014). Systems of high surface area-to-volume ratio such as emulsion with droplet sizes in micrometer range, the evaluation of surface charge on emulsion droplets by ζ-potential measurement is must as it plays an important role in all the electro-kinetic phenomena (Mandal *et al.*, 2012). As discussed earlier negatively charged surfactant molecules accumulate at the oil-water interface forming an electric double layer. The magnitude of electrical charge at the double layer given by ζ-potential determines the aggregation of emulsion droplets, hence the stability. ζ-Potential value of −72.52 mV suggests a good stability with slow phase separation because of the repulsive forces acting at oil-water interface that prevents it coalescence (Khademi *et al.*, 2017). The small emulsion droplets as seen from microscopic image, Figure 10b support this deduction. A conductivity value of 5.12 mS/cm denoted the formation of O/W emulsion, necessary for emulsion to be used as an injection slug into the reservoir. In addition, stability study of optimized emulsion with time was performed by conventional bottle-test method to examine the phase change of the emulsion. As observed from Figure 11, initially a single emulsion phase is visible after proper homogenization of all the phases. The first line of emulsion separation was observed after 3 h. As witnessed the optimized emulsion remained table for more than 5 days before the phases separate out indicating its long term stability. This is attributed to slow re-coalescence phenomenon of oil droplets. The presence of surfactant coating around oil droplets leads to their electrostatic repulsion creating a hindrance for them to re-combine, hence longer stability. Rheological analysis informs about the nature of the emulsion and is crucial for its stability determination. The formulated emulsion showed a non-Newtonian behavior. The reason to pseudo-plastic behavior is already discussed in Section 3.2.4 (a). To reflect the reservoir condition viscosity was also measured at high temperature (70 °C). Figure 12a presents the viscosity curve with rheological parameters (n and k) at 30 °C and 70 °C. Viscosity as a function of temperature decreased with increase in shear rate. Rise in temperature induces increment in vibrations of emulsion droplets due to increase in their thermal energy which leads to cohesive force reduction. Reduction of cohesive force with increase of vibrational energy with reduced time period of contact

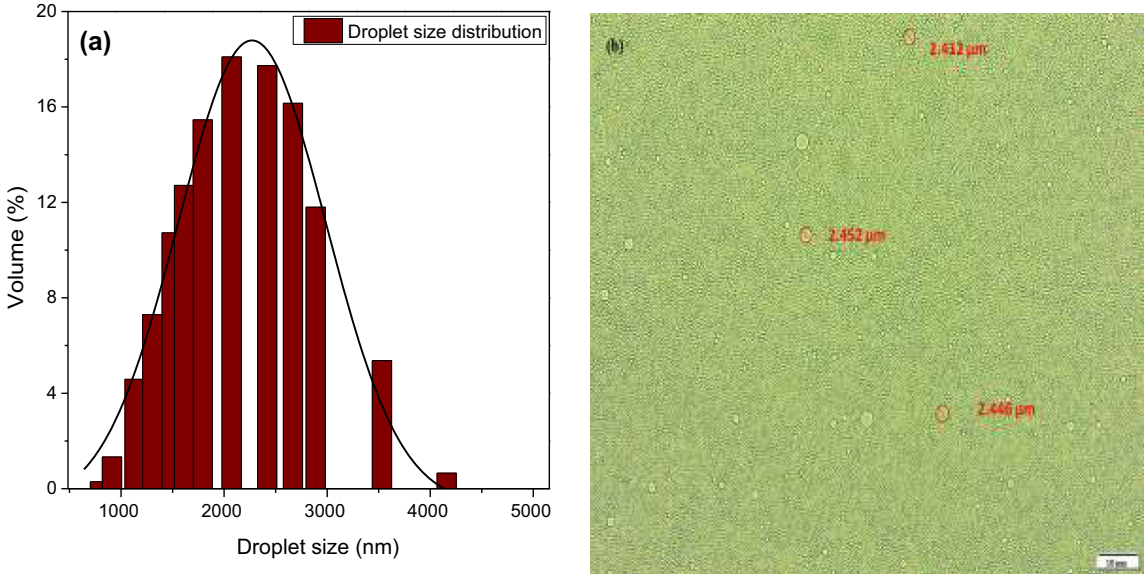

Fig. 10. (a) Droplet size distribution and (b) microscopic image of the optimized emulsion.

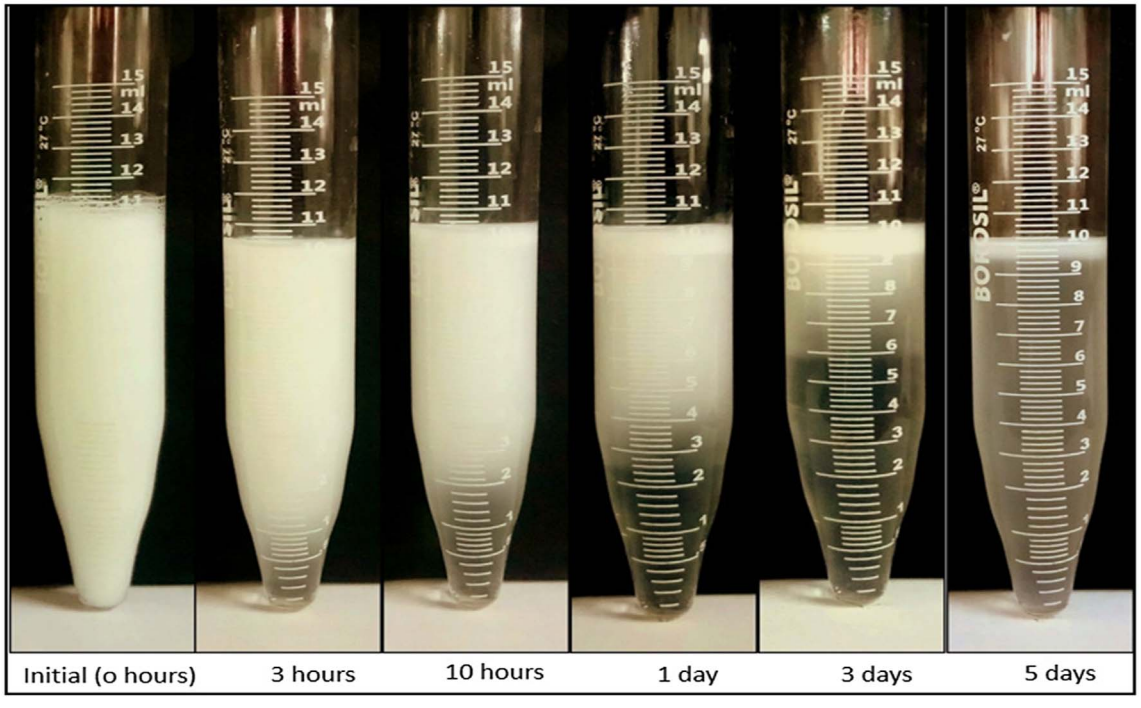

Fig. 11. Phase behavior observation of optimized emulsion at 70 °C at different intervals.

enhances the motion of emulsion droplets. The slippage of surfactant molecules over emulsion droplets due to their loose packing and inter-molecular kinetic energy reduction may also lead to viscosity reduction (Predota *et al.*, 2016). Even though a decrease in viscosity was observed, emulsion viscosity was higher than the conventional chemical slugs (surfactant solution) used in the reservoir for EOR application due to the bi-continuous structure formation. The emulsion should be able to withstand the high shear applied during its injection into the reservoir as breakdown of the bi-continuous structure can lead to its phase separation. Enhancement in viscosity can also be due to the enrichment in structural interactions because of the interconnected water and oil channels (Martins *et al.*, 2016). A high viscosity value of emulsion than conventional slugs will provide better volumetric efficiency during emulsion flooding, thus more oil recovery. The viscoelastic behavior or dynamic moduli of optimized emulsion with varying angular frequency (rad/s) is presented in Figure 12b at 30 °C and 70 °C. G' and G'' were determined by oscillatory

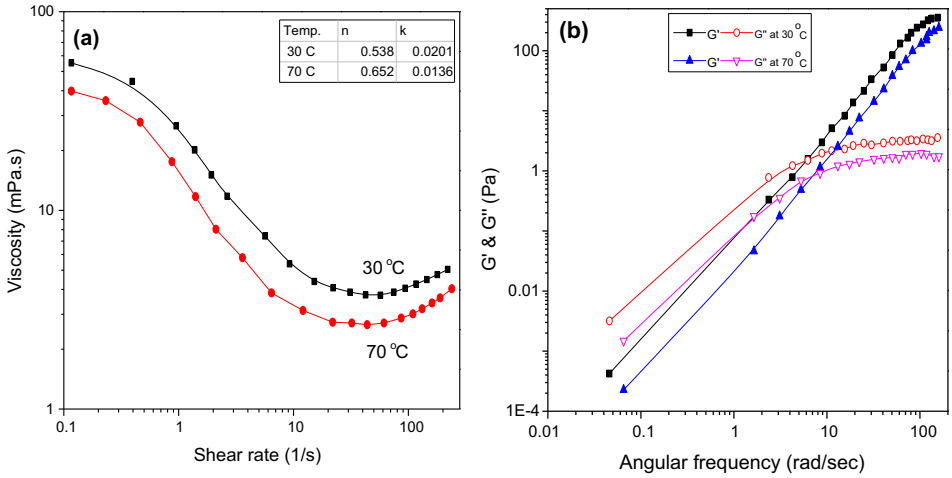

Fig. 12. Viscosity (a) and viscoelastic (b) curves of the optimized emulsion.

experiments. When a fluid deforms its viscoelastic behavior *i.e.*, viscous and elastic nature analysis is necessary. Both G' and G'' rise with increase in angular frequency indicating viscoelastic behavior is possessed by the optimized emulsion. Dominance of G'' over G' ($G' < G''$) at both temperatures in lower angular frequency range suggest viscous nature of the optimized emulsion. Specific Frequency (SF), the intersecting point of G' and G'' signify the point of transition between viscous and elastic nature. An increase in temperature from 30 °C to 70 °C moved SF downwards with a shift towards right suggesting an increase in viscous behavior of emulsion. Temperature rise enhances the mobility of surfactant molecules making emulsion more flowable by reducing the relaxation time (Deng *et al.*, 2015). Dominance of G' over G'' ($G' > G''$) after SF shows the transition from viscous to elastic nature. At low angular frequency below SF viscous nature or G'' dominates the emulsion behavior and after SF elastic nature or G' is the guiding factor. Thus, elastic nature of optimized emulsion is depicted in high angular frequency region because of large values of G' with almost constant values of G''. A better injection of optimized emulsion is indicated by constant values of G''. Wetting behavior study of optimized emulsion aims at enhancing the solubilization of trapped crude oil and its subsequent mobilization from the rock pores. The contact angle of distilled water on crude oil aged quartz specimen at the beginning was found in the range 90°–100°, indicating the specimen surface to be intermediate-wet. Wettability alteration of specimen occurs due to interaction of surfactant molecules present in emulsion with the organic components of the crude oil (Xia *et al.*, 2008). According to Derjaguin and Landau's and Verwey and Overbeek's (DLVO) theory, the formation of a wetting-water film by subsequent adsorption of surfactant coated oil droplets and water molecules over the quartz specimen surface alters the nature of the quartz specimen to water-wet (Standnes and Austad, 2000). The diffusion of surfactant molecules occurs at the crude oil-emulsion interface due to the interfacial tension gradient present between the two fluid phases, discussed as Marangoni effect (Jarrahian *et al.*, 2012). With attachment of surfactant molecules and their formation of water film over the surface of the quartz specimen tends to slowly rollup of the crude oil constituents from the surface (Shramm, 2000). The formed water-film thickness gradually decreases with time because of interaction amid surfactant molecules, crude oil and quartz specimen. Ultimately, detachment of crude oil molecules takes place from the surface with readily solubilization by the injected emulsion that can be squashed effortlessly from the reservoir pore throats (Kao *et al.*, 1988). Figure 13 shows the variation of dynamic contact angle with temperature (30 °C and 70 °C) of the optimized emulsion. An increase in temperature enhances the thermal activity of the adsorbed surfactant stabilized emulsion droplets over the specimen surface. This is due to the reduction in cohesive force of emulsion with rise in temperature leading to lowering of surface tension than the surface energy of the specimen (Kumar and Mandal, 2020). Which in turn causes the emulsion to spread and effectively wet the surface of crude oil aged quartz specimen. The sessile drops of optimized emulsion became highly water-wet from intermediate wet over the quartz specimen surface with time. A decrease in contact angle from 101.35° to 3.42° at 30 °C in 1020 s and from 100.87° to 3.21° at 70 °C in 400 s shows the effect and importance of temperature in wettability alteration as observed from the sessile drop images.

3.5 Miscibility test with crude oil

For the recovery of the trapped crude oil, formulated optimized emulsion must be miscible with the crude oil present in the reservoir. The substance property to fully mix into each other forming a consistent phase is known as miscibility. Formation of *in-situ* emulsions by surfactant slugs during conventional flooding needs high turbulence and large surfactant amount; that also which has very uncertain properties because of its dependence on formation fluid composition. To elude such behavior of *in-situ* emulsion, property evaluation of formulated optimized emulsion is

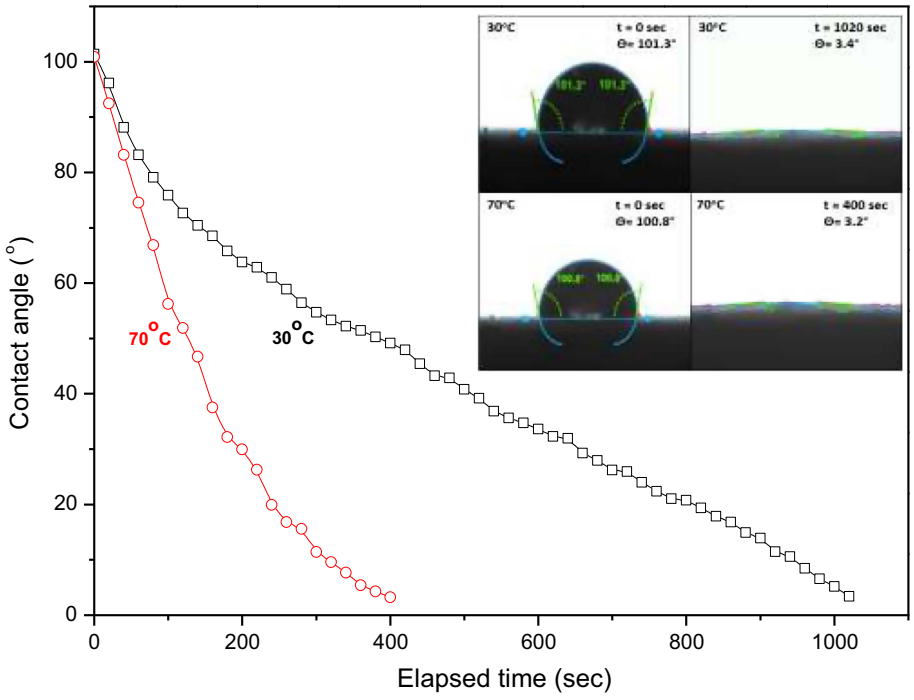

Fig. 13. Dynamic contact angle measurements of the optimized emulsion at 30 °C and 70 °C.

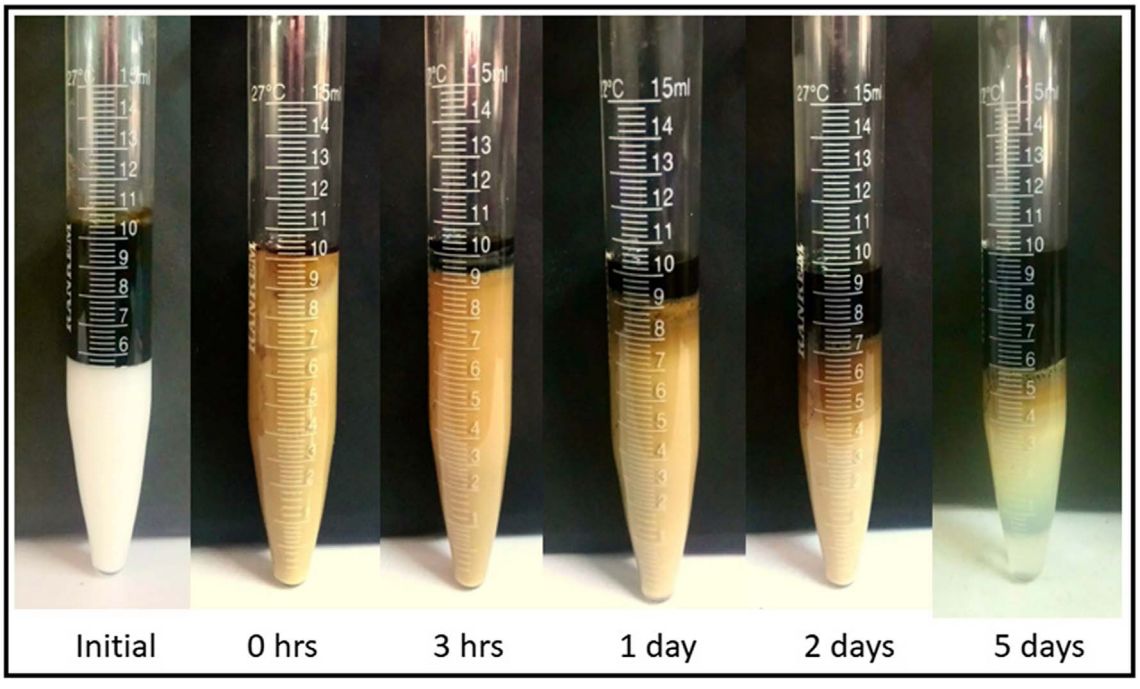

Fig. 14. Dynamic phase behavior analysis of optimized emulsion with crude oil at 70 °C.

required prior to its use as an EOR agent (See *et al.*, 2011). Miscibility behavior of emulsion-crude oil informs about the feasibility of emulsion in the reservoir. Miscibility of optimized emulsion without phase separation to crude oil is important, as phase separation may lead to reservoir pore blockage. Optimized emulsion got instantaneously mixed with the crude oil by thoroughly mixing them for 2 h giving a continuous light brown color mixture. The homogeneous mixture formed was kept for phase separation in a sealed glass tube at 70 °C. Figure 14 shows the dynamic phase behavior study of optimized emulsion-crude oil mixture. The excess oil separates at the top from the mixture with

Table 8. Sandstone core properties with optimized emulsion and polymer flooding results.

Exp. SN. No.	Porosity (%)	Permeability, k (mD)		Design of chemical slug	Secondary recovery (% OOIP)	Additional recovery (% OOIP)	Cumulative Oil recovery (% OOIP)	% Saturation		
		k_w (S_w =1)	k_o (S_{wi})					S_{wi}	S_{oi}	S_{or}
I	25.10	110.21	42.67	Optimized emulsion	54.20	21.03	75.23	16.03	83.97	20.80
II	24.96	109.45	41.82	1.5 wt.% aqueous PHPA	52.92	13.64	66.56	15.57	84.43	28.23

time. The miscibility of crude oil in emulsion is favored by the presence of surfactant (SDS) which lowers the IFT at oil-water interface (Cheraghian, 2015). The oil separation from the homogeneous phase started after 3 h. The crude oil remained solubilized into the mixture for more than 5 days and 3 phases are clearly visible-crude oil at top (black color), separated emulsion at the bottom and emulsified crude in the middle (yellowish brown color). The recovery of oil is decided by the time period for which crude oil remains emulsified into the emulsion *i.e.*, the volume of emulsified crude (yellowish brown color) decides the recovery. High oil solubilization parameter value (V_{os}/V_s = 116.20) with ultralow IFT value (σ_{om} = 2.22E–05 mN/m) at crude oil-middle emulsion phase as compared to that at water-middle emulsion phase (V_{ws}/V_s = 77.46 and σ_{wm} = 4.99E–05 mN/m) as calculated by Chun-Huh equation for the sample after 5 days suggest better solubilization of crude oil by optimized emulsion.

3.6 Oil recovery by optimized emulsion

The oil recovery by optimized emulsion based on the above discussions and its efficiency comparison to a polymer solution was performed on sandstone core. Table 8 presents the sandstone core properties with the flooding results for the optimized emulsion and the aqueous polymer (1.5 wt.% PHPA) solution performed at 70 °C. The irreducible water saturations (S_{wi}) during crude oil flooding in the brine saturated sandstone core equivalent to the Original Oil In Place (OOIP) for the two sets of flooding experiments were calculated as 16.03% and 15.57%, respectively. The water removal by injected crude oil and proper oil ageing permits the formation of an oil-saturated reservoir replica. Figure 15 shows the cumulative oil recovery (%) with water cut (%) for optimized emulsion and aqueous polymer solution. The water flooding accounted for 54.20% and 52.92% of OOIP for the two different experiments. The injection of chemical slugs (optimized emulsion and aqueous polymer solution) into the sandstone core was done when water cut reached to ~100% to maintain the cost-effectiveness of the process (Pal *et al.*, 2019b). Injection of polymer reduces the mobility contrast between displacing fluid and displaced fluid, which leads to improvement in sweep efficiency and hence oil recovery. Whereas, the oil is displaced by three mechanisms in the reservoir-IFT reduction, wettability alteration and emulsification by the injected emulsion. An increase in % oil recovery was observed with rise in injected pore volume of optimized emulsion and polymer solution.

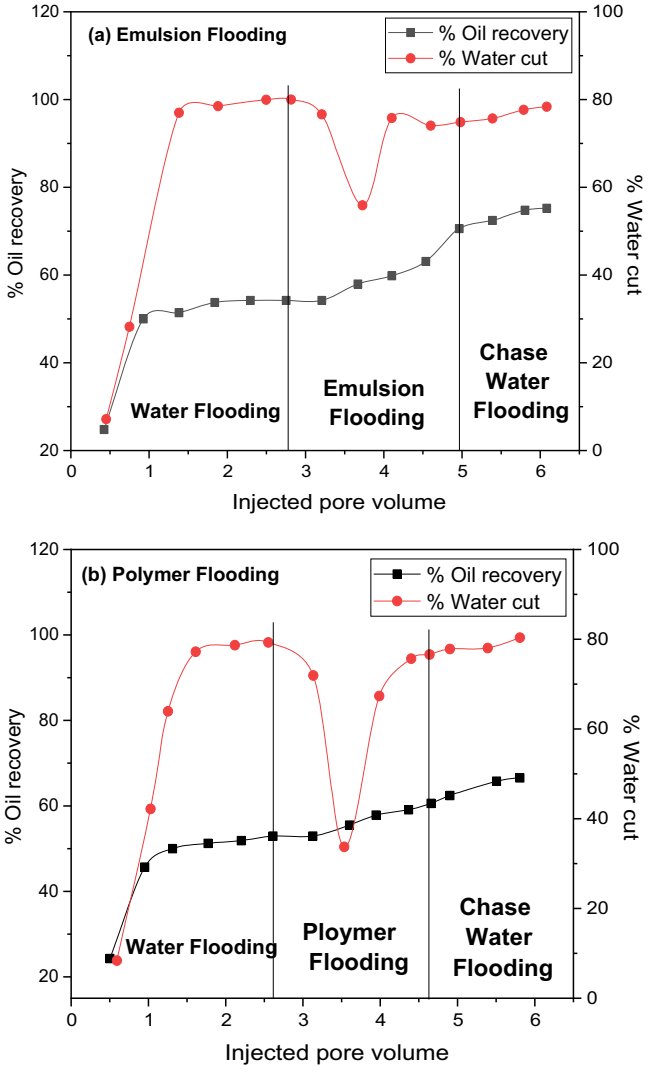

Fig. 15. % Cumulative oil recovery and % water cut as a function of injected pore volume during sandstone core flooding experiments of (a) optimized emulsion and (b) polymer solution.

After water flooding, injection of optimized emulsion and aqueous polymer solution accounted tertiary recoveries of 21.03% of OOIP (Sor of 20.79%) and 13.64% of OOIP (Sor of 28.23%). At the end of chemical slugs injection, chase water flooding was parallelly started aiming to remove the residual crude oil by maintaining the constant

oil bank movement. A cumulative oil recovery of 75.23% of OOIP and 66.56% of OOIP was obtained by optimized emulsion and aqueous polymer solution injection. As observed, from Figure 15 the oil recovery by optimized emulsion is far better than that of aqueous polymer solution. The removal of trapped oil from the minute reservoir pores and prevention from their re-entrapment with enhanced oil emulsification by not letting the back flow of the formed oil bank accounts for the improved oil recovery by the injected optimized emulsion as compared to that for the aqueous polymer solution.

The optimized emulsion thus formed, after characterization evolves as a promising chemical EOR agent recovering crude oil from developed reservoirs with droplet size in micrometer range, IFT reduction ability, wettability alteration capability, enhanced viscosity and miscibility with crude oil. Emulsion injection may require specialized equipment's for emulsion formation compared to surfactant injection. However, emulsion injection promises better oil recovery as indicated from the outcomes of the emulsion characterization and flooding experiment. Emulsion blocks the high permeable zones and recovers oil from fine pores. Surfactant loss by adsorption at rock surfaces is very less in emulsions due to less availability of free surfactant molecules in the dispersed phase. Better mobility control with enhanced oil recovery via large oil bank formation is obtained because of improved rheological behavior by emulsion application. Therefore, emulsion injection can be economically fruitful for longer production time. However, limitations are there in emulsion implementation such as, stability of emulsion, interaction of emulsion with subsurface parameters of reservoirs that vary significantly from location to location, etc. Thus, significant development of emulsion technology is vital depending on condition of actual reservoir. Recently, emulsified acid was used in sandstone reservoirs for EOR application by Shafiq *et al.* (2018). They concluded that emulsified acid is found to have a huge potential in improving the production performance of sandstone reservoir by enhancing porosity and permeability. Moreover, a study also investigated the low salinity EOR potential in high acidic oil fields similar to that from the West of China. They explored the low salinity effect in reservoirs with high acidic components through zeta potential measurements, contact angle and surface modeling (Sari *et al.*, 2019). Therefore, though the optimum values of subsurface parameters (salinity 0.254 wt.%, pH 3.0 and at temperature 30 °C) for optimized emulsion largely vary from an actual oilfield conditions, its application for EOR in field conditions is feasible and justified.

4 Conclusion

Application of emulsion in EOR processes is relatively not new but the studies related to the influence of the subsurface parameters on emulsion behavior are very limited. In the present study, the complex interactions of the independent variables *i.e.*, salinity, pH and temperature on the physiochemical properties of emulsion were successfully investigated. The optimum value selection of the independent variables through their response analysis on droplet size, zeta potential, conductivity and rheological parameters was successfully accomplished by the Taguchi OA generated experimental model with their significance ($p < 0.05$) verification by ANOVA analysis. Obtained results designated salinity (A) to be the critical variable influencing every emulsion property by significant interaction with pH and temperature. Multiple response optimization presented the optimum values of salinity, pH and temperature as 0.254 wt.%, 3.0 and 30 °C respectively with the predicted response values of optimized emulsion properties. With no significant difference between experimental and predicted response the adequacy of the model was justified. Characterization of the optimized emulsion formulated using optimum values of independent variables for enhanced oil recovery was successfully manifested. Explanation of contact angle by DLVO theory with preferential adsorption of emulsion droplets at the quartz surface to form a water-wet film and wettability alteration to water-wet from intermediate-wet because of Marangoni effect. A better mobility control of optimized emulsion is indicated by pseudo-plastic behavior with stable viscosity values over the shear rate range suggesting enhancement in displacement efficiency during its injection. Analysis of G' and G'' *i.e.* viscoelastic behavior indicates transition of viscous to elastic behavior of the optimized emulsion at SF. Ultralow IFT value of 2.22E–05 mN/m and high oil solubilization parameter at crude oil-middle emulsion phase obtained by optimized emulsion implied its better emulsifying capability. Recovery of 21.03% of OOIP was attained after secondary recovery by the injected optimized emulsion. In conclusion, the findings of the study present a fundamental understanding of the complex interactions of independent parameters (pH, temperature and salinity) on the emulsion system and its application for synthesizing a chemical slug for residual oil extraction from matured reservoirs.

Acknowledgments. Authors acknowledge, Central Research Facility (CRF) and Department of Petroleum Engineering of IIT-(ISM) Dhanbad, India for providing the necessary facilities and supporting this study.

Disclosure of potential conflicts of interest

The authors declare that they have no known competing financial interests or personal relationships that could have appeared to influence the work reported in this paper.

References

Acedo-Carrillo J.I., Rosas-Durazo A., Herrera-Urbina R., Rinaudo M., Goycoolea F.M., Valdez M.A. (2006) Zeta potential and drop growth of oil in water emulsions stabilized with mesquite gum, *Carbohydrate Polym.* **65**, 3, 327–336. https://doi.org/10.1016/j.carbpol.2006.01.016.

Aggarwal A., Singh H., Kumar P., Singh M. (2008) Optimizing power consumption for CNC turned parts using response surface methodology and Taguchi's technique – a comparative analysis, *J. Mater. Process. Technol.* **200**, 1–3, 373–384. https://doi.org/10.1016/j.jmatprotec.2007.09.041.

Allen D.R. (1968) Physical changes of reservoir properties caused by subsidence and repressuring operations, *J. Pet. Technol.* **20**, 01. https://doi.org/10.2118/1811-PA.

Allouche J., Tyrode E., Sadtler V., Choplin L., Salager J.L. (2004) Simultaneous conductivity and viscosity measurements as a technique to track emulsion inversion by the phase-inversion-temperature method, *Langmuir* **20**, 2134–2140. https://doi.org/10.1021/la035334r.

Al-Zahrani S.M., Al-Fariss T.F. (1998) A general model for the viscosity of waxy oils, *Chem. Eng. Process* **37**, 5, 433–437. https://doi.org/10.1016/S0255-2701(98)00047-6.

Amanullah Md., Al-Tahini A.M. (2009) Nano-technology-its significance in smart fluid development for oil and gas field application, in: *SPE Saudi Arabia Section Technical Symposium*, SPE 126102-MS, Society of Petroleum Engineers. https://doi.org/10.2118/126102-MS.

Amirpour M., Shadizadeh S.R., Esfandyari H., Ahmadi S. (2015) Experimental investigation of wettability alteration on residual oil saturation using nonionic surfactants: Capillary pressure measurement, *Petroleum* **1**, 289–299. https://doi.org/10.1016/j.petlm.2015.11.003.

Bezerra M.A., Santelli R.E., Oliveira E.P., Villar L.S., Escaleira L.A. (2008) Response Surface Methodology (RSM) as a tool for optimization in analytical chemistry, *Talanta* **76**, 5, 965–977. https://doi.org/10.1016/j.talanta.2008.05.019.

Binks B.P. (1998) Emulsions-recent advances in understanding, in *Modern aspects of emulsion science* (Chapter 1), B.P. Binks (ed), Royal Society of Chemistry, Cambridge, UK. https://doi.org/10.1039/9781847551474-00001.

Cheraghian G. (2015) An experimental study of surfactant polymer for enhanced heavy oil recovery using a glass micromodel by adding nanoclay, *Pet. Sci. Technol.* **33**, 1410–1417. https://doi.org/10.1080/10916466.2015.1062780.

Clifford P.J., Sorbie K.S. (1985) The effects of chemical degradation on polymer flooding, SPE-13586-MS, in: *SPE Oilfield and Geothermal Chemistry Symposium*, Society of Petroleum Engineers. https://doi.org/10.2118/13586-MS.

Deng L., Que F., Wei H., Xu G., Dong X., Zhang H. (2015) Solubilization of tea seed oil in a food-grade water-dilutable microemulsion, *PLoS One* **10**, 5, e0127291. https://doi.org/10.1371/journal.pone.0127291.

Dong H.Z., Fang S.F., Wang D.M., Wang J.Y., Liu Z., Hong B. H. (2008) Review of practical experience & management by polymer flooding at Daqing, in: *SPE Symposium on Improved Oil Recovery, Tulsa, Oklahoma, USA*, SPE 114342, Society of Petroleum Engineers, https://doi.org/10.2118/114342-MS.

Egbogah E.O., Dawe R.A. (1981) Spontaneous emulsification aspect of enhanced oil recovery, in: *32nd Annual Technical Meeting*, Calgary, Preprint, Petroleum Society of Canada. https://doi.org/10.2118/81-32-40.

Farouq-Ali S.M. (1976) Non-thermal heavy oil recovery methods, in: *SPE Rocky Mountain Regional Meeting*, SPE 5893-MS, Society of Petroleum Engineers. https://doi.org/10.2118/5893-MS.

Gäbler A., Wegener M., Paschedag A., Kraume M. (2006) The effect of pH on experimental and simulation results of transient drop size distributions in stirred liquid–liquid dispersions, *Chem. Eng. Sci.* **61**, 3018–3024. https://doi.org/10.1016/j.ces.2005.10.072

Garti N., Slavin Y., Aserin A. (1999) Surface and emulsification properties of a new gum extracted from *Portulaca oleracea* L, *Food Hydrocoll.* **13**, 2, 145–155. https://doi.org/10.1016/S0268-005X(98)00082-4.

Golnabi H., Matloob M.R., Bahar M., Sharifian M. (2009) Investigation of electrical conductivity of different water liquids and electrolyte solutions, *Iranian Phys. J.* **3**, 2, 24–28. https://www.sid.ir/en/journal/ViewPaper.aspx?*ID*=191551.

Griffin W.C. (1949) Classification of Surface-Active Agents by "HLB", *J. Soc. Cosmet. Chem.* **1**, 5, 311–326. http://journal.scconline.org/contents/cc1949/cc001n05.html.

Harnsilawat T., Pongsawatmanit R., McClements D.J. (2006) Influence of pH and ionic strength on formation and stability of emulsions containing oil droplets coated by â-Lactoglobulin-alginate Interfaces, *Biomacromolecules* **7**, 2052–2058. https://doi.org/10.1021/bm050656q.

Hibbert D.B. (2012) Experimental design in chromatography: a tutorial review, *J, Chromatogr. B Anal. Technol. Biomed. Life Sci.* **910**, 2–13. https://doi.org/10.1016/j.jchromb.2012.01.020.

Huang X., Kakuda Y., Cui W. (2001) Hydrocolloids in emulsions: particle size distribution and interfacial activity, *Food Hydrocoll.* **15**, 4–6, 533–542. https://doi.org/10.1016/S0268-005X(01)00091-1.

Hunter R.J. (1986) *Foundations of colloid science*, Oxford University Press, Oxford, UK.

Hunter R.J. (1998) Recent developments in the electroacoustic characterization of colloidal suspensions and emulsions, *Colloids Surf. A Physicochem. Eng. Aspects* **141**, 1, 37–66. https://doi.org/10.1016/S0927-7757(98)00202-7.

Jafari S.M., Assadpoor E., He Y., Bhandari B. (2008) Re-coalescence of emulsion droplets during high-energy emulsification, *Food Hydrocoll.* **22**, 7, 1191–1202. https://doi.org/10.1016/j.foodhyd.2007.09.006.

Jarrahian K., Seiedi O., Sheykhan M., Sefti M.V., Ayatollahi S. (2012) Wettability alteration of carbonate rocks by surfactants: a mechanistic study, *Colloids Surf. A* **410**, 1–10. https://doi.org/10.1016/j.colsurfa.2012.06.007.

Jiao J., Burgess D.J. (2003) Ostwald ripening of water-in-hydrocarbon emulsions, *J. Colloid Interface Sci.* **264**, 2, 509–516. https://doi.org/10.1016/S0021-9797(03)00276-5.

Jourdain L., Leser M.E., Schmitt C., Michel M., Dickinson E. (2008) Stability of emulsions containing sodium caseinate and dextran sulfate: Relationship to complexation in solution, *Food Hydrocoll.* **22**, 647–659. https://doi.org/10.1016/j.foodhyd.2007.01.007.

Kanan K., Al-Jabari M., Kayali I. (2017) Phase behavioral changes in SDS association structures induced by cationic hydrotropes, *Arab. J. Chem.* **10**, S314–S320. https://doi.org/10.1016/j.arabjc.2012.08.003.

Kang H.S., Kwon S.S., Kim B.H., Lee B.R., Kang K.H., Hong J.E., Han S.H., Chang I.S. (2002) Nanoemulsion as a vitamin E acetate carrier to enhance infiltration into oral mucous membrane, *J. Indus. Eng. Chem.* **8**, 348–353. https://www.cheric.org/research/tech/periodicals/view.php?seq=384318KW.

Kao R.L., Wasan D.T., Nikolov A.D., Edwards D.A. (1988) Mechanisms of oil removal from a solid surface in presence of anionic micellar solutions, *Colloids Surf.* **34**, 4, 389–398. https://doi.org/10.1016/0166-6622(88)80163-X.

Karnanda W., Benzagouta M.S., AlQuraishi A., Amro M.M. (2013) Effect of temperature, pressure, salinity, and surfactant concentration on IFT for surfactant flooding optimization, *Arab. J. Geosci.* **6**, 9, 3535–3544. https://doi.org/10.1007/s12517-012-0605-7.

Karthikeyan S., Jeeva P.A., Jerobin J., Mukherjee A., Chandrasekaran N. (2012) Formulation and characterization of nanoemulsion coatings from *Azadirachta indica*, *Int. J. ChemTech Res.* **4**, 4, 1566–1570.

Khademi M., Wang W., Reitinger W., Barz D.P.J. (2017) Zeta potential of poly (methylmethacrylate) (PMMA) in contact with aqueous electrolyte-surfactant solutions, *Langmuir* **33**, 40, 10473–10482. https://doi.org/10.1021/acs.langmuir.7b02487.

Kumar N., Gaur T., Mandal A. (2017) Characterization of SPN Pickering emulsions for application in enhanced oil recovery, *J. Ind. Eng. Chem.* **54**, 304–315. https://doi.org/10.1016/j.jiec.2017.06.005.

Kumar N., Mandal A. (2018a) Oil-in-water nanoemulsion stabilized by polymeric surfactant: Characterization and properties evaluation for enhanced oil recovery, *European Polym. J.* **109**, 265–276. https://doi.org/10.1016/j.eurpolymj.2018.09.058.

Kumar N., Mandal A. (2018b) Surfactant stabilized oil-in-water nanoemulsion: stability, interfacial tension, and rheology study for enhanced oil recovery application, *Energy Fuels* **32**, 6, 6452–6466. https://doi.org/10.1021/acs.energyfuels.8b00043.

Kumar N., Mandal A. (2018c) Thermodynamic and physicochemical properties evaluation for formation and characterization of oil-in-water nanoemulsion, *J. Mol. Liq.* **266**, 147–159. https://doi.org/10.1016/j.molliq.2018.06.069.

Kumar N., Mandal A. (2020) Wettability alteration of sandstone rock by surfactant stabilized nanoemulsion for enhanced oil recovery – A mechanistic study, *Colloids Surf. A* **601**, 125043. https://doi.org/10.1016/j.colsurfa.2020.125043.

Lee K.S. (2011) Performance of a polymer flood with shear-thinning fluid in heterogeneous layered systems with cross-flow, *Energies* **4**, 8, 1112–1128. https://doi.org/10.3390/en4081112.

Leong T.S.H., Wooster T.J., Kentish S.E., Ashokkumar M. (2009) Minimising oil droplet size using ultrasonic emulsification, *Ultrason. Sonochem.* **16**, 721–727. https://doi.org/10.1016/j.ultsonch.2009.02.008.

Mandal A., Bera A., Ojha K., Kumar T. (2012) Characterization of surfactant stabilized nanoemulsion and its use in enhanced oil recovery, *Soc. Pet. Eng.* **6**, 537–542. https://doi.org/10.2118/155406-MS.

Martins M.A., Neves C.M., Kurnia K.A., Carvalho P.J., Rocha M.A., Santos L.M., Freire M.G. (2016) Densities, viscosities and derived thermos-physical properties of water saturated imidazolium-based ionic liquids, *Fluid Phase Equilib* **407**, 188–196. https://doi.org/10.1016/j.fluid.2015.05.023.

Mason R.L., Gunst R.F., Hess J.J. (2003) *Statistical design and analysis of experiments with applications to engineering and science*, John Wiley and Sons Inc., An International Thomason Publishing, Europe, London, 1V7AA, Hoboken, NJ.

McClements D.J. (2004) Protein-stabilized emulsions, *Curr. Opin. Colloid Interface Sci.* **95**, 305–313. https://doi.org/10.1016/j.cocis.2004.09.003.

Montgomery D.C. (2013) *Design and analysis of experiments*, 8th edn., John Wiley & Sons Inc, Hoboken, NJ. https://lccn.loc.gov/2017002355.

Moreira de Morais J., Henrique dos Santos O.D., Delicato T., Azzini Goncalves R., Alves da Rocha-Filho P. (2006) Physicochemical characterization of canola oil/water nano-emulsions obtained by determination of required HLB number and emulsion phase inversion methods, *J. Dispersion Sci. Technol.* **27**, 1, 109–115. https://doi.org/10.1081/DIS-200066829.

Ohshima H., Makino K. (2014) *Colloid and interface science in pharmaceutical research and development*, Elsevier.

Pal N., Kumar N., Verma A., Ojha K., Mandal A. (2018) Performance evaluation of novel sunflower oil-based gemini surfactant(s) with different spacer lengths: application in enhanced oil recovery, *Energy Fuels* **32**, 11344–11361. https://doi.org/10.1021/acs.energyfuels.8b02744.

Pal N., Kumar N., Mandal A. (2019a) Stabilization of dispersed oil droplets in nanoemulsions by synergistic effects of the gemini surfactant, PHPA polymer, and silica nanoparticle, *Langmuir* **35**, 7, 2655–2667. https://doi.org/10.1021/acs.langmuir.8b03364.

Pal N., Kumar N., Saw R.K., Mandal A. (2019b) Gemini surfactant/polymer/silica stabilized oil-in-water nanoemulsions: Design and physicochemical characterization for enhanced oil recovery, *J. Pet. Sci. Eng.* **183**, 106464. https://doi.org/10.1016/j.petrol.2019.106464.

Park J., Lee S., Lee J.W. (2018) Effect of pH and concentrated salt on the droplet size and mass transfer coefficient in a stirred liquid-liquid reactor, *Ind. Eng. Chem. Res.* **57**, 6, 2310–2321. https://doi.org/10.1021/acs.iecr.7b04793.

Pei H., Zhang G., Ge J., Tang M., Zheng Y. (2012) Comparative effectiveness of alkaline flooding and alkaline-surfactant flooding for improved heavy-oil recovery, *Energy Fuels* **26**, 5, 2911–2919. https://doi.org/10.1021/ef300206u.

Predota M., Machesky M.L., Wesolowski D.J. (2016) Molecular origins of the zeta potential, *Langmuir* **32**, 40, 10189–10198. https://doi.org/10.1021/acs.langmuir.6b02493.

Sakthivel S., Velusamy S., Gardas R.L., Sangwai J.S. (2015) Adsorption of aliphatic ionic liquids at low waxy crude oil-water interfaces and the effect of brine, *Colloids Surf. A* **468**, 62–75. https://doi.org/10.1016/j.colsurfa.2014.12.010.

Sari A., Chen Y., Xie Q., Saeedi A. (2019) Low salinity water flooding in high acidic oil reservoirs: Impact of pH on wettability of carbonate reservoirs, *J. Mol. Liq.* **281**, 444–450. https://doi.org/10.1016/j.molliq.2019.02.081.

See C.H., Saphanuchart W., Looi M.H., Loke Y.S. (2011) Crude oil recovery from sludge treated by nanoemulsion composition, SPE-145935-MS, in: *SPE Asia Pacific Oil and Gas Conference and Exhibition*, Society of Petroleum Engineers. https://doi.org/10.2118/145935-MS.

Shafiq M.U., Chong Y.J., Mahmud H.K.B., Hossain M.M., Rezaee R., Testamanti N. (2018) Application of emulsified acids on sandstone formation at elevated temperature conditions: an experimental study, *J. Pet. Explor. Prod. Technol.* **9**, 1323–1329. https://doi.org/10.1007/s13202-018-0567-8.

Shramm L.L. (2000) *Surfactants: Fundamentals and applications in the petroleum industry*, 1st edn., Cambridge University Press, New York.

Standnes D.C., Austad T. (2000) Wettability alteration in chalk: 2. Mechanism for wettability alteration from oil-wet to water-wet using surfactants, *J. Pet. Sci. Eng.* **28**, 123–143.

Terry R.E., Rogers J.B. (2014) *Applied Petroleum Reservoir Engineering*, third edition, Pearson Education, 528 p.

Tiab D., Donaldson E.C. (2004) *Petrophysics: Theory and Practice of Measuring Reservoir Rock and Fluid Transport Properties*, 2nd edn., Elsevier, New York, USA, pp. 313–414.

Xia H., Wang D., Wang G., Ma W., Deng H.W., Liu J. (2008) Mechanism of the effect of micro-forces on residual oil in chemical flooding, in: *SPE Symposium on Improved Oil Recovery, 20-23 April, Tulsa, Oklahoma, USA*, Society of Petroleum Engineers. https://doi.org/10.2118/114335-MS.

Xu H., Liu Y., Zhang L. (2015) Salting-out and salting-in: competitive effects of salt on the aggregation behavior of soy protein particles and their emulsifying properties, *Soft Matter* **11**, 5926–5932. https://doi.org/10.1039/C5SM00954E.

Yuan C.D., Pu W.F., Wang X.C., Sun L., Zhang Y.C., Cheng S. (2015) Effects of interfacial tension, emulsification, and surfactant concentration on oil recovery in surfactant flooding process for high temperature and high salinity reservoirs, *Energy Fuels* **29**, 6165–6176. https://doi.org/10.1021/acs.energyfuels.5b01393.

Zhang Z., Li J., Zhou J. (2011) Microscopic roles of "Viscoelasticity" in HPMA polymer flooding for EOR, *Transp. Porous Media* **86**, 199–214. https://doi.org/10.1007/s11242-010-9616-6.